Spatial Temperature Uniformity and

Statistical Determination of Dominant Degradation Modes in PV Modules

by

Neelesh Umachandran

A Thesis Presented in Partial Fulfillment
of the Requirements for the Degree
Master of Science

Approved July 2015 by the
Graduate Supervisory Committee:

Govindasamy Tamizhmani, Co-Chair
Liping Wang, Co-Chair
Patrick Phelan

ARIZONA STATE UNIVERSITY

August 2015

ABSTRACT

This is a two-part thesis.

Part 1 of this thesis investigates the influence of spatial temperature distribution on the accuracy of performance data of photovoltaic (PV) modules in outdoor conditions and provides physical approaches to improve the spatial temperature distribution of the test modules so an accurate performance data can be obtained in the field. Conventionally, during outdoor performance testing, a single thermocouple location is used on the backsheet or back glass of a test module. This study clearly indicates that there is a large spatial temperature difference between various thermocouple locations within a module. Two physical approaches or configurations were experimented to improve the spatial temperature uniformity: thermally insulating the inner and outer surface of the frame; backsheet and inner surface of the frame. All the data were compared with un-insulated conventional configuration. This study was performed in an array setup of six modules under two different preconditioning electrical configurations, Voc and MPPT over several clear sunny days. This investigation concludes that the best temperature uniformity and the most accurate I-V data can be obtained only by thermally insulating the inner and outer frame surfaces or by using the average of four thermocouple temperatures, as specified in IEC 61853-2, without any thermal insulation.

Part 2 of this thesis analyzes the field data obtained from old PV power plants using various statistical techniques to identify the most influential degradation modes on fielded PV modules in two different climates: hot-dry (Arizona); cold-dry (New York). Performance data and visual inspection data of 647 modules fielded in five different

power plants were analyzed. Statistical tests including hypothesis testing were carried out to identify the I-V parameter(s) that are affected the most. The affected performance parameters (Isc, Voc, FF and Pmax) were then correlated with the defects to determine the most dominant defect affecting power degradation. Analysis indicates that the cell interconnect discoloration (or solder bond deterioration) is the dominant defect in hot-dry climate leading to series resistance increase and power loss, while encapsulant delamination is being the most dominant defect in cold-dry climate leading to cell mismatch and power loss.

To,

Suneetha Umachandran, Kattavarapalli Umachandran (my mom and dad) and my other family members for their constant love and support. Also to my dearest friend Rajyalakshmi for her never ending care and motivation to whom I owe part of my success in all that I do.

ACKNOWLEDGMENTS

Firstly, my deepest gratitude is to my thesis advisor, Dr. Govindasamy Tamizhmani (Mani), for accepting me into the lab to work as a part of his research group and for his constant guidance and support in all possible ways. It was fortunate and a great inspiration to work with such a hardworking person. I would also like to thank my committee members, Dr. Liping Wang and Dr. Patrick Phelan, for their time and serving on my thesis committee.

I would also like to thank Dr. Joseph Kuitche, our lab manager for his guidance and knowledge he imparted during this work. My special thanks goes to Sai Tatapudi, our lab technical manager for his constant support during experiments and motivation during my work at PRL. I also thank Bulent Bicer, our project manager who helped coordinating with us for our field visits and managing our projects.

Lastly, I am extremely grateful to be able to work with a group of individuals, who are hardworking, helpful and with deep passion to learn and innovate. I would like to thank Christopher Raupp, Matthew Chicca, Sravanthi Boppana, Mathan Kumar Moorthy, Vidyashree Rajasekar, Pooja Jagadeesan and Sanjay Shrestha for their support. I should mention, the amount of knowledge I gained by discussions and meetings played a very important part during my work at PRL.

The funding from Solar Energy Institute for India and United States of DOE (SERIIUS/DOE), Salt River Project (SRP) and Electric Power Research Institute (EPRI) for the project is truly acknowledged.

TABLE OF CONTENTS

Page

LIST OF TABLES

LIST OF FIGURES

Figure Page

Figure Page

NOMENCLATURE

PV - Photovoltaic

STC - Standard test conditions (T_{mod} = 25°C; Irradiance = 1000 W/m^2; AM = 1.5)

AM – Air Mass

Isc – Short-circuit

Voc – Open-circuit voltage

Imp – Maximum current

Vmp – Maximum voltage

Pmax – Maximum power

MPPT – Maximum peak power tracking

Rs – Series resistance

Rsh – Shunt resistance

PART 1: SPATIAL TEMPERATURE UNIFORMITY IN A PV MODULE

1.1 INTRODUCTION

1.1.1 Background

A photovoltaic (PV) module temperature depends on irradiance, material properties, and electrical configuration. Also, temperature of a PV module heavily depends on thermal equilibrium between the heat generated in the module and the heat lost to environment due to conduction, convection and radiation. Conduction heat transfer takes place between various materials of a module packaging, convection happens between surface of a module and the moving air around, and radiation happens between the module surfaces to the sky and the ground. Also, with respect to performance, irradiance on a module directly affects the current while voltage is affected by temperature. Generally, for crystalline silicon modules, voltage decreases by 1% for every 2.5°C rise in temperature or -0.4%/°C and power decreases by 1% for every 2.2°C rise in temperature or -0.45%/°C. Thereby, temperature plays an important role in performance of a PV module. Usually, module performance is usually reported at standard test conditions (STC) as per ASTM 1036 – 15 [1] for module comparison and selection by system designers and energy modelers, while field operating conditions deviate widely from STC. Ambient temperature and irradiance varies widely time to time in field that directly affects module temperature thereby influencing the performance of a module. Temperature changes are taken into account in terms of module temperature coefficients as per the module datasheet provided by the manufacturer. Hence, predicting

the module performance in field operating conditions has to be more accurate considering all the variability in temperature.

1.1.2 **Statement of the Problem**

Predominantly, temperature coefficients are arrived based on indoor solar simulator results where the conditions are controlled, but a module in field operates in varying ambient conditions and the temperature coefficients obtained using solar simulator may not represent “true” coefficients. Considering this issue, the IEC standards committee released a standard IEC 61853-1 [2] which requires a power (Pmax) matrix containing Pmax measurements at seven irradiance levels and four different temperatures either indoor or outdoor. When generating this Pmax matrix outdoor using natural sunlight, practical difficulties with respect to temperature and irradiance changes influence our measurements. Irradiance has less variation on a clear sunny day in places like Arizona, but the temperature has wide variations and it’s a challenge to maintain uniform temperature within a module. Factors such as wind, clouds, physical irregularities due to module components and mounting can significantly affect temperature uniformity.

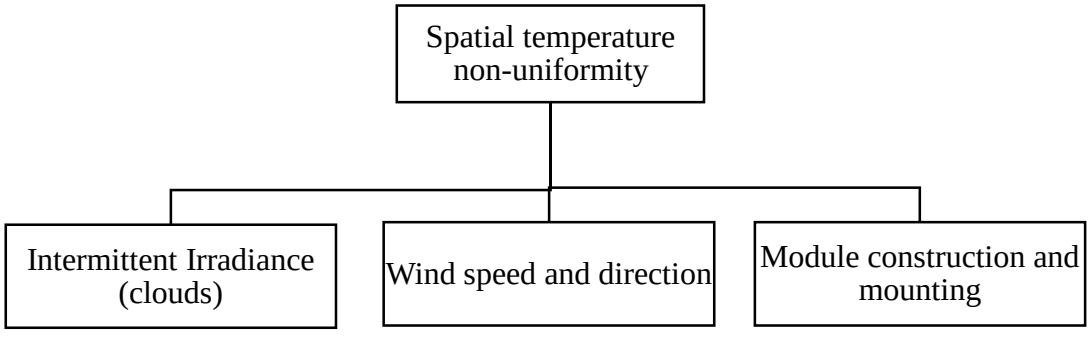

Figure 1. Spatial temperature non-uniformity

This study attempts to reduce temperature anomalies due to module construction and mounting by thermally insulating module frames and back surfaces at various electrical configurations and quantify the effect of insulation in terms of accuracy in module I-V characteristics.

1.1.3 **Scope of the work**

Scope of this work includes,

- Short – period temperature monitoring (~ 1 hour) of modules at various electrical configurations (Isc, Voc and MPPT) and insulation configurations (backsheet, frame, both backsheet and frame) to analyze the influence of different combinations on temperature uniformity.
- Installing six modules on fixed tilt rack with two identical modules each having same insulation type for temperature measurement.
- Setting up multi-curve tracer and data logger for continuous performance measurement of all the modules at MPPT and for continuous temperature data collection at four locations in each module respectively.
- Temperature monitoring of modules in long – term (2 – 3 days) mounted on fixed tilt rack at Voc and Pmax in three different insulation methods (no insulation; frame insulated; frame and backsheet insulated) to analyze the repeatability and effectiveness of thermal insulation on temperature uniformity.
- Analysis on temperature data to identify the configuration that has least temperature variability by comparing with the un-insulated module at all electrical configurations.

- Quantifying temperature variability within a module based on I-V parameters collected continuously on modules mounted on fixed tilt rack.
- Baseline test to obtain temperature coefficients of all the modules on the rack simultaneously using a multi-curve tracer and comparing the deviation in temperature coefficients due to non-uniform temperature distribution within a module.

1.2 **LITERATURE REVIEW**

1.2.1 **Influence of temperature on module performance**

The effect of temperature on performance and reliability of PV modules is well documented by multiple authors. Solar cells, which are semiconductor materials have high dependence on temperature. A direct influence of temperature on a semiconductor properties is decrease in band gap and increase in minority carrier lifetime. These effects on semiconductor properties helps slight increase in Isc, but exponential decrease in saturation current [3]. Also, increase in temperature leads to decrease in Voc which is at relatively higher rate than increase in Isc and eventually leading to efficiency losses [4]. Considering this effect on modules where cells are connected in series, it is crucial to analyze the temperature variation within a module that directly affects power output.

1.2.2 **Module temperature uniformity**

Temperature uniformity is of prime importance in order to accurately predict the module I-V parameters in field operating conditions and also to determine the temperature coefficients of I-V parameters (Isc, Imp, Voc, Vmp, and Pmax). Module I-V parameters can be determined either indoor or outdoor, inaccuracies in indoor temperature measurements can be less compared to temperature measurements outdoor due to practical field conditions. In any given module installed outdoor, there will be cell-t-cell temperature differences within a module. In a study done with seven module samples outdoor, it was identified that there is approximately about 2 K cell-to-cell temperature differences [5]. K. Emery *et al.* identified various methods to achieve wide range of module temperatures with more uniformity and measure module characteristics during indoor testing [6]. During outdoor testing, anomalies in temperature non-

uniformity in a module can influence temperature coefficient measurements and is illustrated by D. L. King *et al.* [7]. Module frame can make the edge cells relatively cooler than center cells and also the cell(s) above the junction box can be hotter than other cells. Thermally insulating the frames and back surface can isolate the module from environmental influences and other temperature irregularities thereby we could accurately predict module performance and temperature coefficients [7].

1.2.3 **Temperature measurement**

Measuring temperature of a module accurately is very important during performance characterizations and predicting energy yield. Measurement inaccuracies can be caused either because of temperature drop between cell and back surface in account to thermal conductivity and also due to lack of thermal equilibrium [8]. In addition to environmental influence to temperature uniformity, accuracy in performance characterization can be affected by transient conditions between back surface and sensor during temperature ramp up and cool down of a module [6]. Therefore, module temperature sensors should be located carefully and temperature uniformity is investigated after the module(s) reach thermal equilibrium. In this work, multiple sensors are attached on back surface of the module(s) based on the draft standard IEC 61853-2 [9] to obtain a more accurate module temperature and to visualize temperature uniformity within a module. Also, electrical parameters and temperatures were analyzed after the modules attained thermal equilibrium.

Another factor that needs to be considered during temperature monitoring is the operating condition of the module. Module operates at different temperature regimes at different operating conditions. It is demonstrated that module at Voc has about 5° C

difference in T_{mod} - T_{amb} between open-circuit and MPPT condition [10]. ASU and TÜV Rheinland PTL did a study on the effect of electrical configuration on NOCT [11]. The study concluded that open-circuit condition had about 3° C higher NOCT values than resistive load condition.

1.2.4 **Temperature uniformity for outdoor performance testing at ASU**

ASU –PTL developed a thermal test bed (TTB) to obtain outdoor energy ratings of a module in wide range of temperature measurements of about 5° C - 60° C under controlled temperature environment with [12]. Another study at ASU-PTL improved temperature uniformity using phase change material on the backsheet of the module but it was time consuming [13].

This study is approached at different physical methods to improve temperature uniformity by using thermal insulation that can be imparted with the current outdoor performance characterization techniques in a simple manner and for the ease of repeatability. Also, this study investigates the influence of temperature non-uniformity on I-V parameters of a PV module.

1.3 **METHODOLOGY**

1.3.1 **Approach**

This study is approached to improve temperature uniformity based on experimenting with following two factors in different combinations,

1. Thermal Insulation
2. Electrical configuration

Temperature monitoring was done in two phases for this study. Phase - I consists of tests done in short-term (~ 1 hour) at various insulation and electrical configurations on two identical modules and then the worst case combinations were neglected for phase-II. Phase – II incudes long-term temperature monitoring for six identical modules with different insulation configurations installed on open-rack fixed at latitude tilt. Module temperature distribution is obtained by using multiple temperature sensors attached on backsheet of the test modules. Comparative analyses was done on the temperature differences between various temperature sensors in a module at various combinations to an un-insulated module. These temperature differences were then correlated with the measured I-V parameters to investigate the influence of temperature non-uniformity on the accuracy of performance data.

1.3.2 **Test modules**

Different modules were used for both phase-I and II. Module specifications, technology and construction of these modules are discussed below,

1.3.2.1 **Modules – short-term temperature monitoring**

Two ‘identical’ modules were used for all the combinations of insulation and electrical configuration in short-term monitoring in order to neglect temperature

differences because of module quality. Table 1 below are the specifications of the modules used for this study.

Table 1

Module specifications for short-term temperature monitoring

	Technology	Construction	Rated power
Module – A	Poly-Si	Glass/EVA/cell/EVA/polymer	220 W
Module – B	Poly-Si	Glass/EVA/cell/EVA/polymer	245 W

1.3.2.2 **Modules – long-term temperature monitoring**

Six unstressed modules with two identical modules for each insulation configurations was used in this phase of the work. Modules were from five different manufacturers and the specifications are given below in table 2. Modules were selected such that they are of similar module construction, rating and cell dimensions.

Table 2

Module nameplate specifications for short-term temperature monitoring

Name	Module Technology[##]	Insulation type	Isc[#]	Voc[#]	Imp[#]	Vmp[#]	Pmax[#]
Module 1	Mono - Si	No insulation	8.52	44.7	7.96	35.8	285
Module 2	Mono - Si	No insulation	8.36	44.64	7.77	36.72	285
Module 3	Poly - Si	Frame insulation	8.46	44.4	7.81	36.5	285
Module 4	Poly - Si	Frame insulation	8.35	44.5	7.84	36.36	285
Module 5	Poly - Si	Frame and back surface insulation	8.3	44	7.75	35.5	275
Module 6	Poly - Si	Frame and back surface insulation	8.3	44	7.75	35.5	275

- Nameplate values specified by the manufacturer

- All the modules had “Glass/EVA/cell/EVA/polymer” type module construction

1.3.3 **Data acquisition systems**

Various sensors were used to obtain module and ambient data during the tests. Temperature being the prime data variable, factors such as irradiance, ambient temperature and wind speed were also measured to analyze the impact of various factors on temperature distribution.

Irradiance sensor: A pyranometer (Kipp and Zonen) was used to measure plane of array (POA) irradiance. It was mounted on a weather station 15 feet away from the test set-up in latitude tilt (33°S). Also, a reference cell mounted co-planar to the array modules was used for irradiance values during translation of I-V curves to STC.

Wind sensor: An ultrasonic wind sensor was used to measure the wind speed (horizontal). It is mounted on the same weather station and it has a range of about 0 – 60 m/s

Data logger: Data from these sensors are sampled and stored every 1 minute intervals in a Campbell scientific CR 1000 data logger. These data were retrieved from the logger periodically for data analysis.

Temperature Measurement: Temperature measurements are done using multiple T-type thermocouples attached to the backsheet of the module using thermal tape. Manufacturer specified accuracy for these thermocouples is +/- 1°C or 0.75% for temperatures above 0°C. T-type thermocouples were selected for our measurements considering its faster response and wide range of operation.

Temperature sensors are connected to a HOBO 4 – channel thermocouple data logger. Temperature logger stores the data in its memory and can be retrieved periodically. The data is collected in 1 minute intervals with the sampled data of every 5s. Manufacturer claims the accuracy to be ±0.6°C and a range of -260°C TO 400°C. HOBO is a very convenient device for long-term monitoring as it can withstand various environmental conditions and its ease of data collection and retrieval.

Figure 2. HOBO 4 –channel temperature data logger (Source: onset)

1.3.3.1 **Location of temperature sensors**

Temperature sensors are attached in such a way that all the areas in a module is accounted for and an overall module temperature is measured. Determining module operating temperature considering ambient conditions is a part of a draft IEC standard 61853-2 [9], in which sensors are located in the following locations on the back surface of a module.

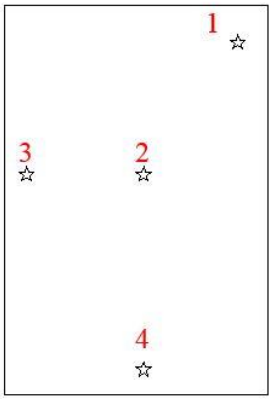

Figure 3. Temperature sensors location per IEC 61853-2 (draft)

1 – Corner; 2 – Center; 3 – Long edge; 4 – Short edge

Location of sensors are named in analysis as shown above. In addition to these locations, temperature sensors were placed in four other locations as shown in figure 4 to analyze the effect of insulation methods on cells close to the frame (edge cells) of a module. But, for the rest of the analysis, only four thermocouples as shown in figure 3 were used.

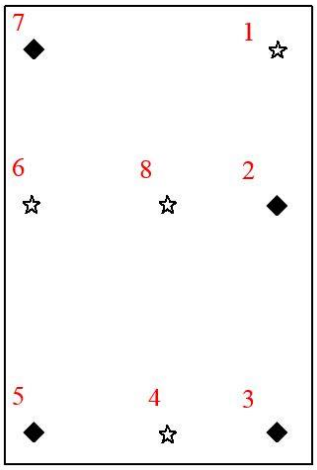

Figure 4. Temperature sensors location for short – term temperature monitoring

☆ - Sensors as per IEC standard ◆ - Additional sensors

1.3.4 **Thermal Insulation**

Thermal insulation was done on frame and backsheet of the module in the three combination combinations so as to reduce the temperature difference due to module

physical irregularities. Since frame is a metal (aluminum), it tends to keep the edge cells cooler and also the cell above junction box can have higher temperatures. Following insulation configurations were done on the modules to compare and identify the insulation method that helps in maintaining temperature uniformity the most within a PV module.

1. No insulation
2. Frame insulation
3. Back surface insulation
4. Frame and back surface insulation

Thermal insulation on module frame was done using a self-sealing R-1 foam insulation tape. This was selected for its ease of installation on module frame and compatibility with the frame structure. Module back surface was insulated using a foam insulation board with R- value of 9.6. This insulation has the highest R-value per inch for a rigid foam board. Insulation was cut for module dimensions and attached to the back surface. This insulation was also used on the inner surface of the module frame.

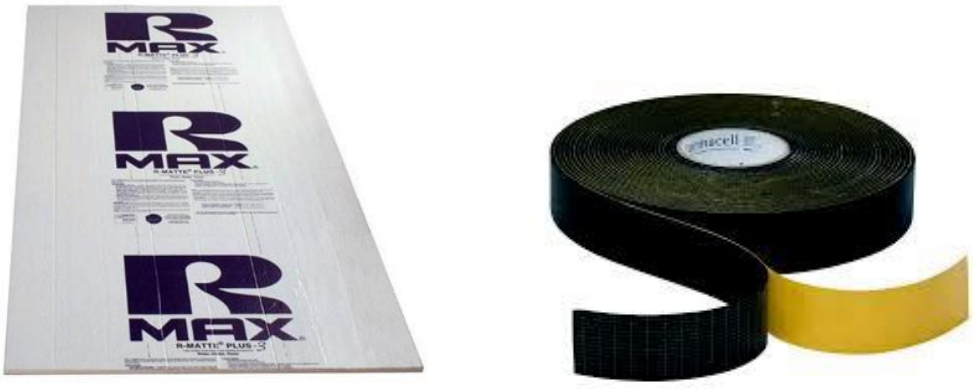

Figure 5. Insulation materials for modules

Thickness of insulation was basically calculated based on the width of the module frame such that the insulation fits perfectly to the backsheet of the module. The thickness of insulation used here for the study was about 1.5 inches.

1.3.4.1 **Insulation configurations**

Modules were insulated in various configurations and the temperature distribution was visualized using multiple temperature sensors attached to the backsheet of the modules. Figures 6 – 10 shown below are the various insulation configurations experimented in a module to neglect temperature variation within a module due to physical irregularities (frame, junction box).

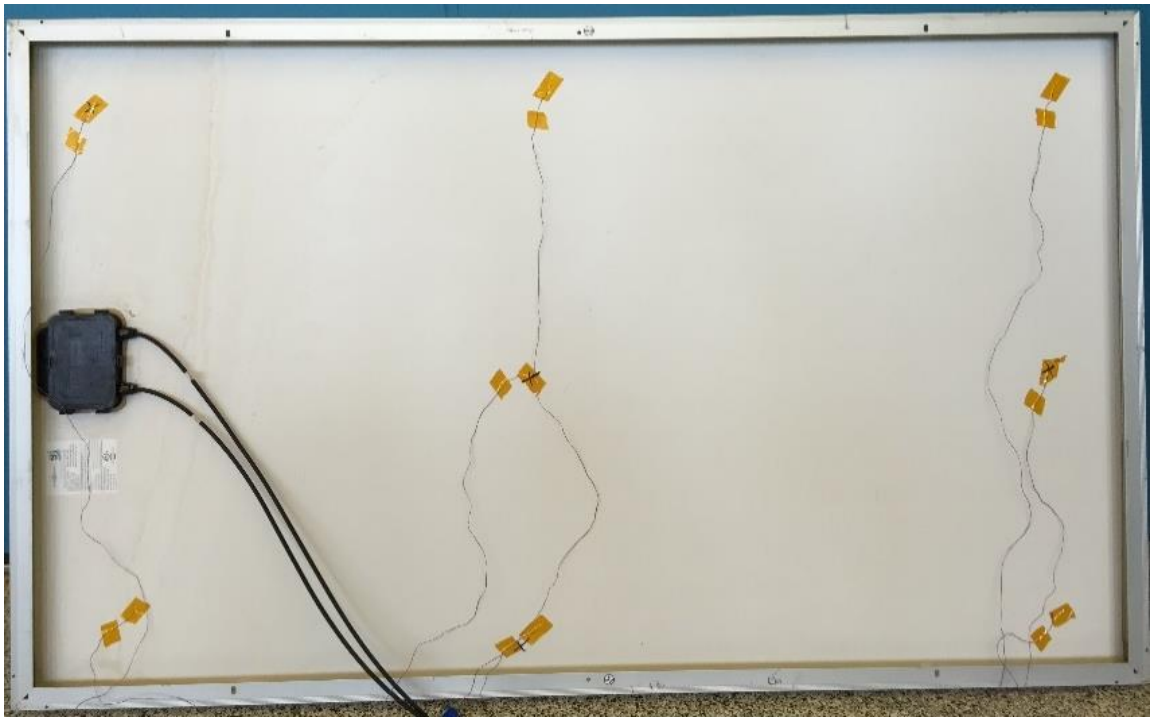

Figure 6. Module with no insulation

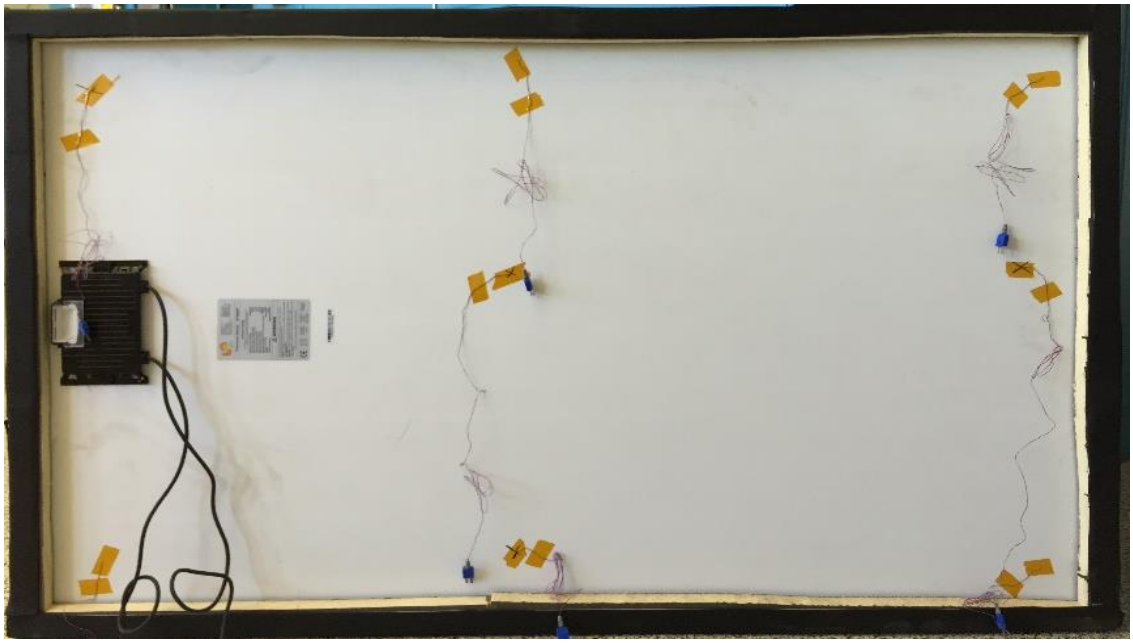

Figure 7. Module with frame insulation

Frame is insulated both on the inner surface and the outer surface. Outer surface of the frame is insulated using an R-1 insulation foam tape while the inner surface was insulated with a rigid foam board cut to appropriate dimensions of the frame.

Figure 8. Frame insulation – inner and outer surface

Figure 9. Module with back surface insulation

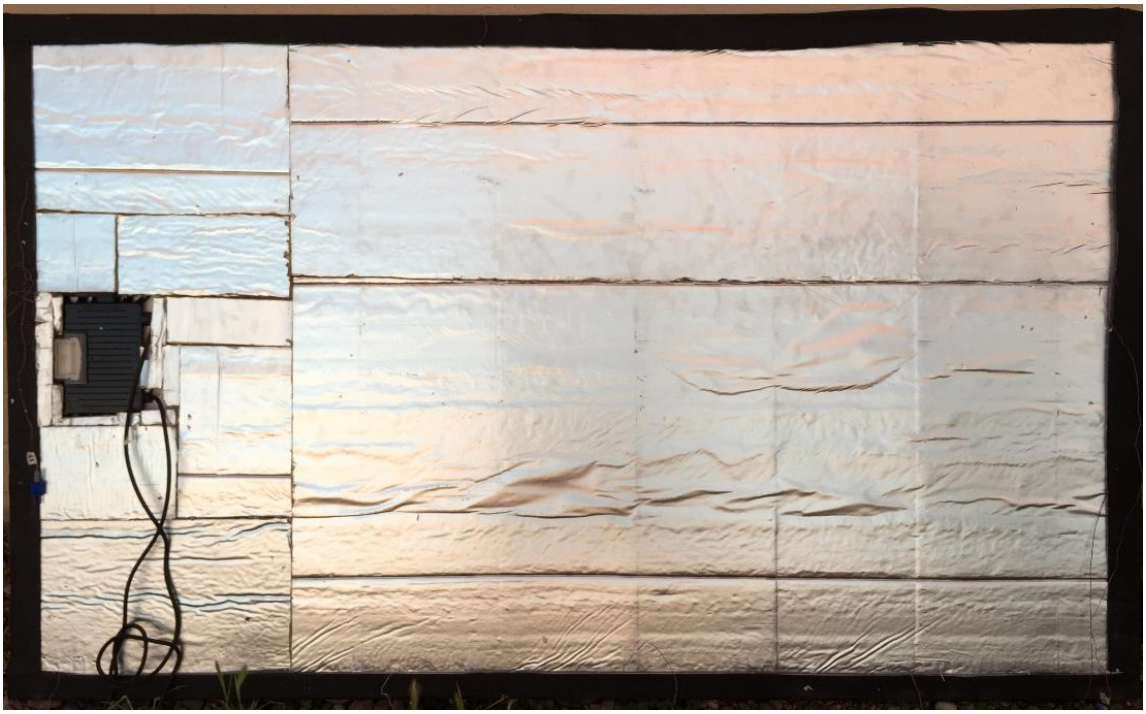

Figure 10. Module with frame and back surface insulation

1.3.5 **Electrical configurations**

Modules were tested with the above mentioned insulation configurations in three different electrical configurations possible in a PV module.

Open-circuit condition (Voc): A module in open-circuit means the voltage across the module is maximum and the current is zero. Open-circuit condition is one when the module leads are not connected.

Short-circuit condition (Isc): A module in short-circuit conditions means there is no voltage across the module. Short-circuit is one when the module leads are connected together without any load.

Maximum power point tracking (MPPT): A module is tracked for maximum power continuously using a daystar MT5 multi-curve tracer. It adjusts the voltage based on the power generated from a module. Multi-curve tracer can measure performances of 16 modules at a time. The tracer is set such that it takes I-V curves every 5 minutes.

The flow chart below represents the different phases of this work and also the steps involved in the experimental procedure.

1.3.6 **Test Procedure**

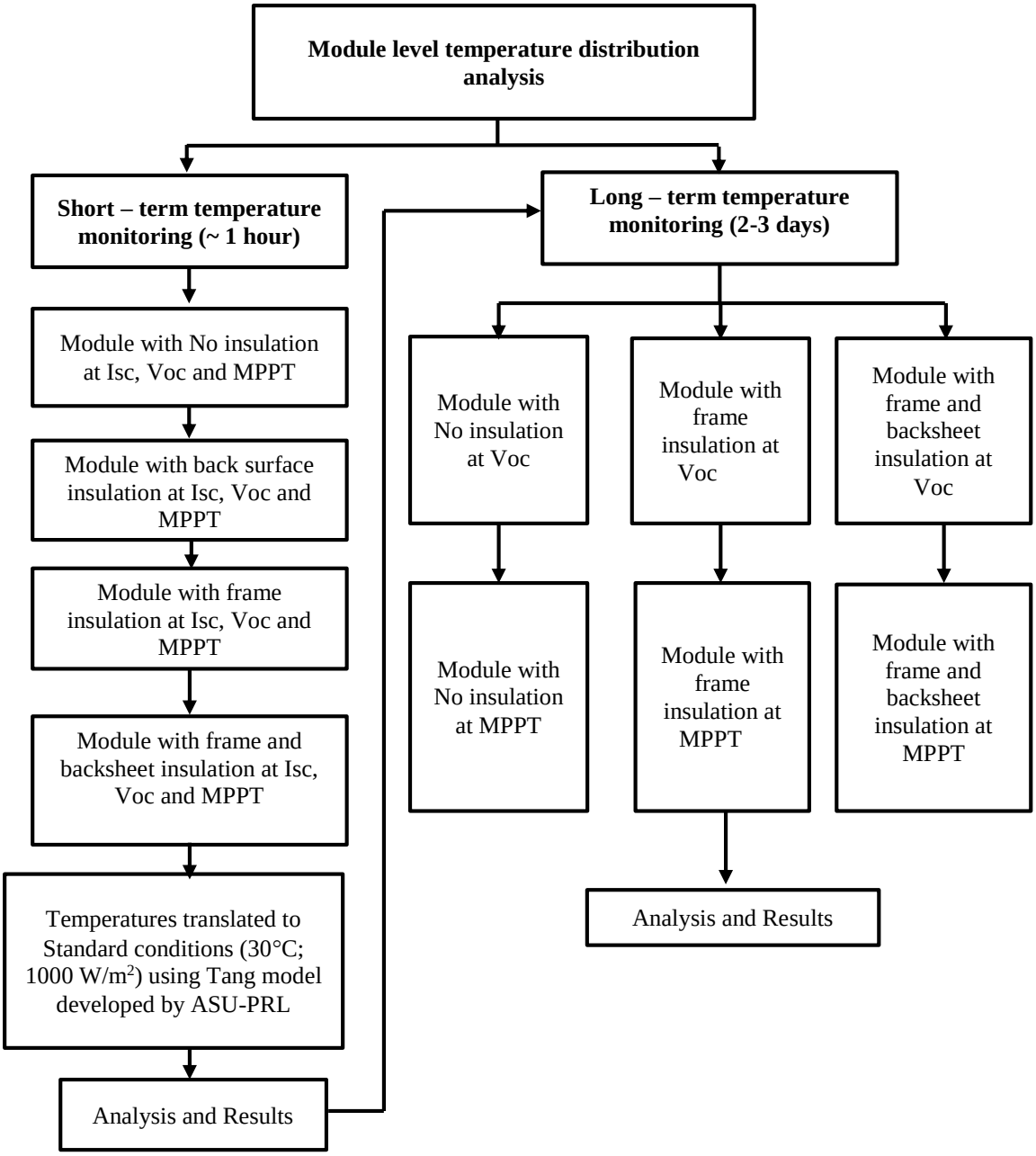

Figure 11. Test Procedure for temperature measurement

1.3.7 **Effect of frame Insulation on edge cells**

Spatial temperature variations or temperature gradients along the surface of a module is primarily caused by change in heat transfer rates between the cells, module components (frame, junction box) and surrounding environment. This issue was addressed by insulating a module at different boundaries (frame, back surface) to control heat transfer rates thereby maintaining uniform temperatures. As an initial test, module frame was insulated and the temperature distribution of eight cells close to the frame was monitored to see the effect of thermal insulation. Figure 12 shows an un-insulated module with temperature sensors on the edge cells and figure 13 shows a frame insulated module with temperature sensors on the edge cells for this test.

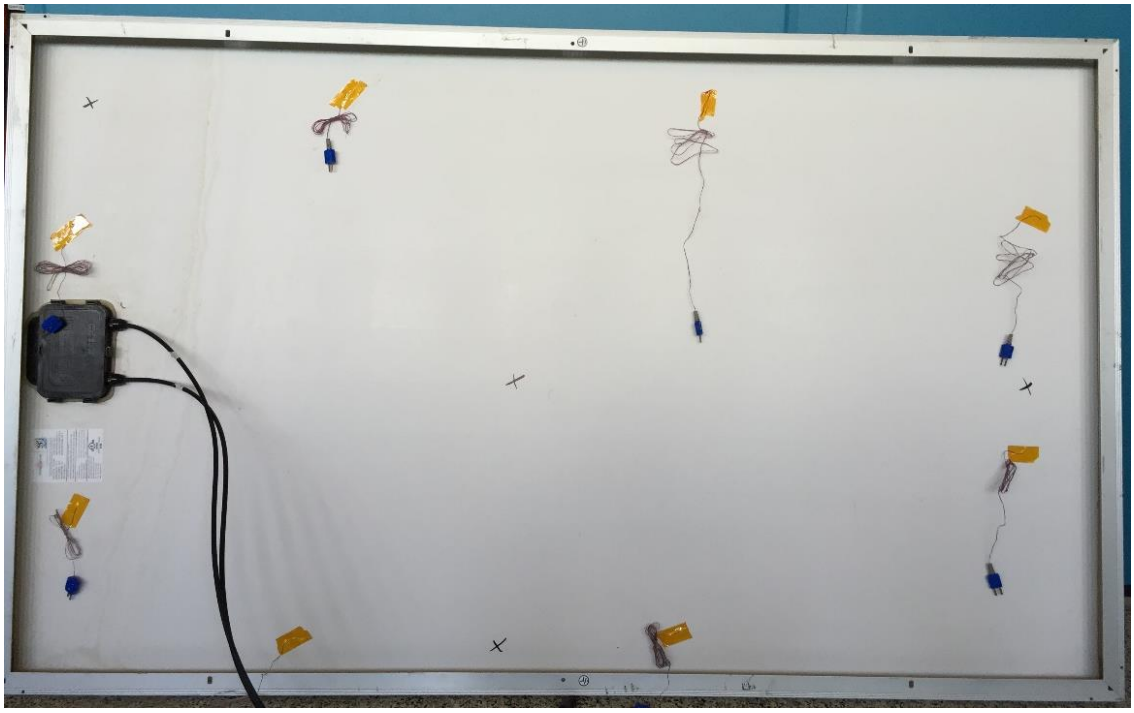

Figure 12. Un-insulated module with sensors on edge cells

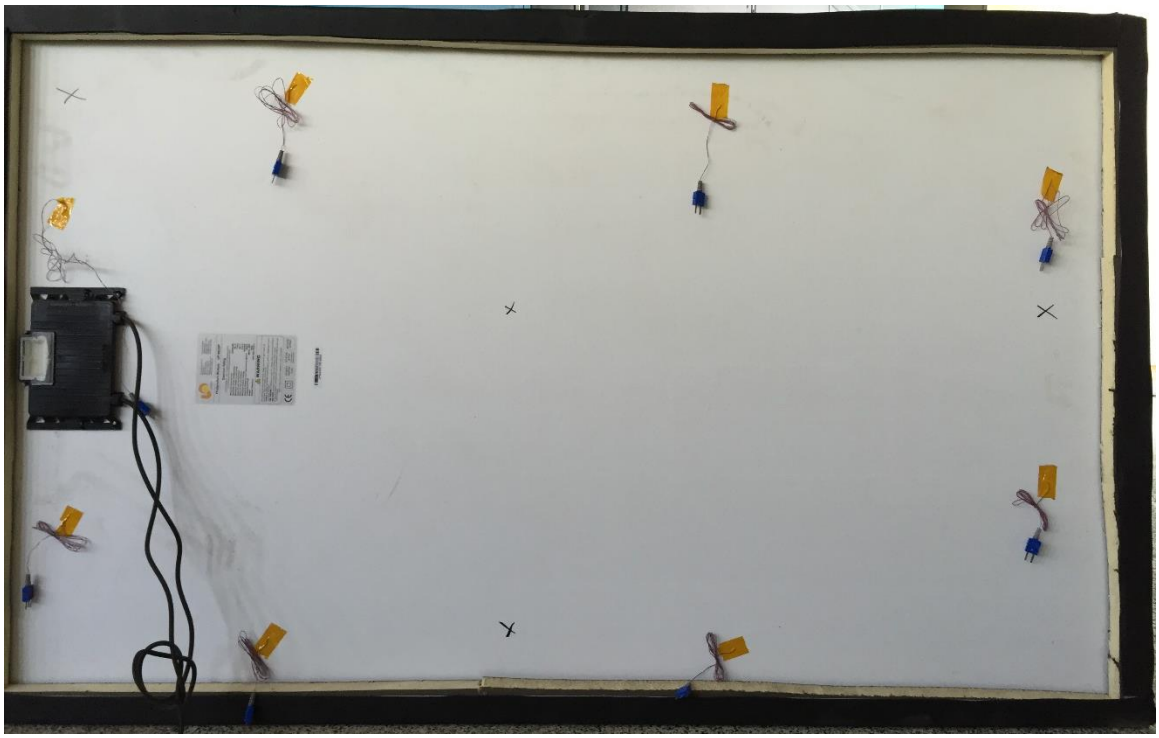

Figure 13. Frame insulated module with sensors on edge cells

Modules were mounted on a movable 1-axis tracker facing south at latitude tilt (33°S) for two hours and temperature data was collected every 30 seconds using a HOBO-4 channel data logger.

1.3.8 **Individual temperature coefficients measurement**

Baseline I-Vs were done on all array modules to obtain temperature coefficients for all I-V parameters before insulation and installation. These temperature coefficients would be used for I-V translation from measured conditions to standard test conditions (STC). A step-by-step procedure to do the test is given below,

i. Cool the module in a chamber to about 5 - 10°

ii. Attach temperature sensor (in the center cell) to the back surface of the module, when it is inside the cooling chamber.

iii. Set-up a movable 1-axis tracker as show in Figure 14 normal to the sun. This is done by adjusting the tracker based on the shadow of the sun dial mounted on the tracker.

iv. A portable Daystar I-V tracer is used to trace the curves. A portable thermometer is used to measure the ambient temperature and the module temperature sensor is connected to the I-V tracer. A matched reference cell is used to measure the irradiance and is also connected to the I-V tracer.

v. Once the set-up is ready, the module is placed on the tracker and then as the module warms up I-V curves are taken. Simultaneously irradiance, ambient temperature and module temperature are recorded with the curve.

vi. Now, T_{mod} vs I_{sc} is plotted, temperature coefficient for I_{sc} is determined similarly, when temperature is plotted with V_{oc}, I_{mp}, V_{mp} and P_{max} respective temperature coefficients are calculated.

The values of temperature coefficients of all modules obtained from this test are presented in APPENDIX A.

1.3.9 **Short-term temperature monitoring**

In phase – I of this work, modules were monitored for short – periods approximately 1 hour for each combination of insulation and electrical loading. An ideal sized module was selected and the temperature was monitored for all combinations. Modules were put at latitude tilt (33°S) for all tests. This tilt was selected because modules would be mounted in an array in the same orientation for long-term temperature monitoring and inferences made from this phase would be carried to the next phase. Also, most of the modules in commercial power plants are always mounted towards south (in

northern hemisphere) close to their respective latitudes. Irradiance, wind speed and ambient temperature was measured from an on-site weather station located about 15 feet away from the tracker. Also, the series of tests for temperature monitoring were done on different days at acceptable prevailing weather conditions (mostly on clear sky days when irradiance > 900 W/m^2).

Given below are a series of steps that were followed for temperature monitoring.

1. A movable 1 – axis tracker was set a latitude tilt 33°S.
2. Module with temperature sensors attached at locations shown in section 1.3.3.2
3. Module was first tested on un-insulated module at open-circuit condition (Voc) for 1 hour with all the temperature sensors attached to HOBO 4-channel data logger. Module is allowed to cool down to room temperature after the test by placing it indoor.
4. Similarly, module was tested with no insulation at short-circuit condition (Isc) by shorting the module leads, this test was done for 30 minutes because loading a module in short-circuit for longer time might damage the module. Temperature sensors were attached to the module and connected to HOBO 4-channel data logger. Then the module was allowed to cool down to room temperature.
5. Module was then tested at maximum power tracking condition (MPPT) by connecting the module to a Daystar MT5 multi-tracer set at peak load for 1 hour. Temperature sensors were attached to HOBO 4-channel data logger.

6. Steps 3 – 5 were repeated for module with backsheet insulation using a rigid foam insulation board cut to appropriate size. Once this was done, backsheet insulation was removed.
7. Steps 3 – 5 were repeated for module with frame insulation using a foam insulation tape.
8. Steps 3 – 5 were repeated for module with frame and backsheet insulation.

Results from phase ‑ I was used to remove a few insulation configurations for the next phase of this work.

Figure 14. Module with frame and backsheet insulation - front and back view

Figure 15. Data logger set-up for short-term monitoring

Since, all the tests were done on different days which had different ambient conditions. All the temperature data was translated to standard conditions of T_{amb} = 30°C, POA Irradiance = 1000 W/m^2 and wind speed = 1 m/s. This was done based on an empirical equation developed from a study collaboratively done by ASU-PTL and NREL [14] for multiple module technologies. Appropriate equation based on module technology was used and modified accordingly.

$$\text{Poly-Si: } T_{translated} = T_{measured} + \{(30 - T_{amb\text{-}measured}) \times 0.926\} + \{(1000 - Irr_{measured}) \times 0.030\} + \{(1 - WS_{measured}) - 1.666\} + 5.1 \quad (1)$$

$$\text{Mono- Si: } T_{translated} = T_{measured} + \{(30 - T_{amb\text{-}measured}) \times 0.942\} + \{(1000 - Irr_{measured}) \times 0.028\} + \{(1 - WS_{measured}) - 1.509\} + 3.9 \quad (2)$$

Once all the temperatures were translated, the differences between various temperature sensors were calculated and then analyzed. Although, temperature differences are not much affected by translation it was done to have a consistent data sets for analyses.

1.3.10 **Long-term temperature monitoring**

Module Installation: Six identical modules were selected based on the size and rated power of the module. Modules are mounted in landscape orientation on the fixed tilt rack at 33°S located at ASU – PRL, Mesa, Arizona. In addition to these six modules, two modules were mounted on both the rear ends of the array so that test modules experience the same thermal environment and any temperature fluctuations due to module position and wind is neglected. Modules were mounted after the insulation on these modules are done and the temperature sensors are attached to the back surface. Figure 16 and 17 show the front view and back of the installed modules on an open rack.

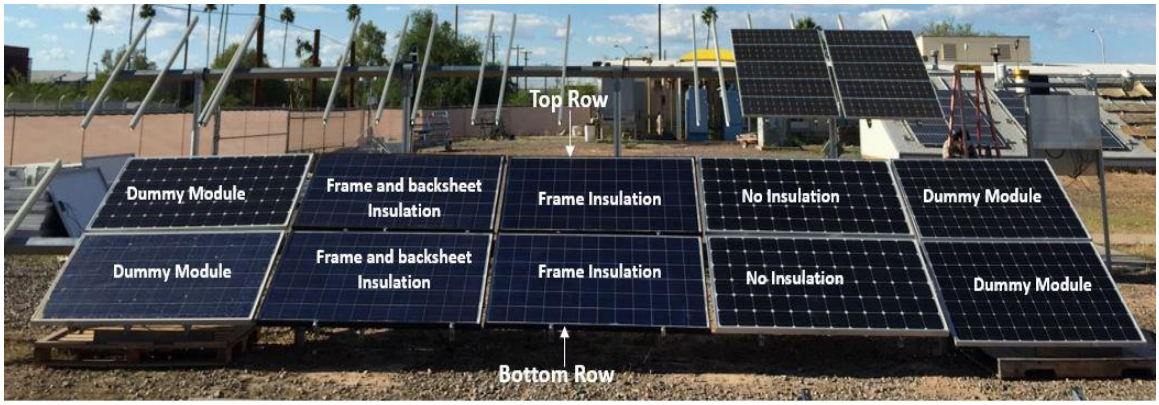

Figure 16. Modules mounted on open rack fixed at 33°S – Front View

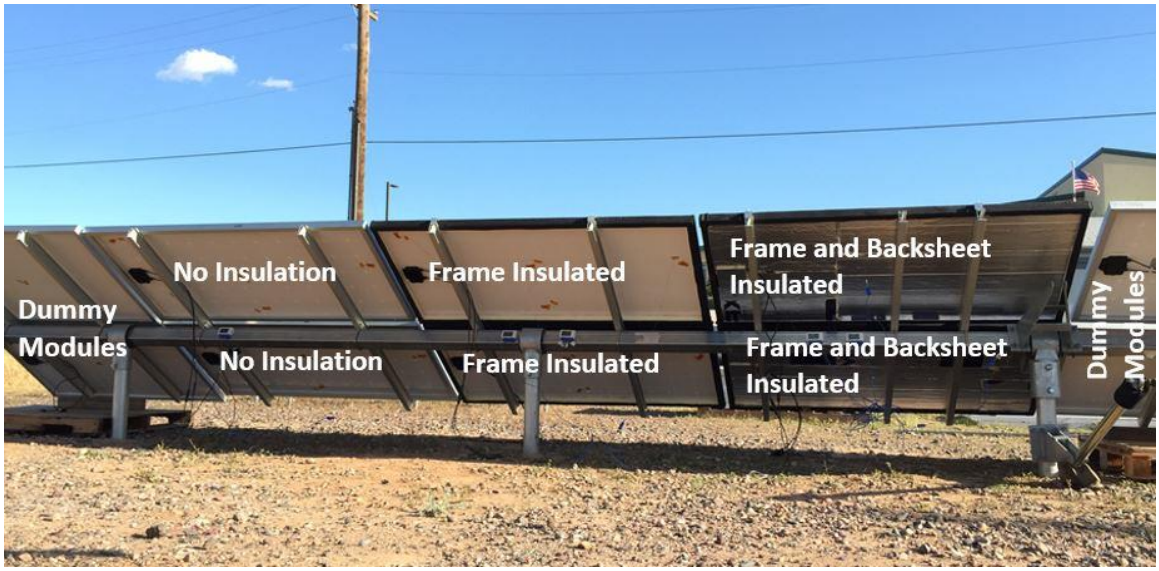

Figure 17. Modules mounted on open rack fixed at 33°S – Back View

Data collection: Module temperature was measured using four temperature sensors attached to the backsheet of the module at locations as shown in Figure 3.

In long-term temperature monitoring, the temperature data was collected for three consecutive clear days at both open-circuit (Voc) and peak power tracking condition (MPPT). All four temperature sensors were attached to a HOBO 4-channel data logger. The temperature data was sampled and collected in 1 minute intervals. Weather data such as POA irradiance, ambient temperature and wind speed were collected from a weather

station close to the array. Figure 18 shows a weather station with different sensors mounted on it.

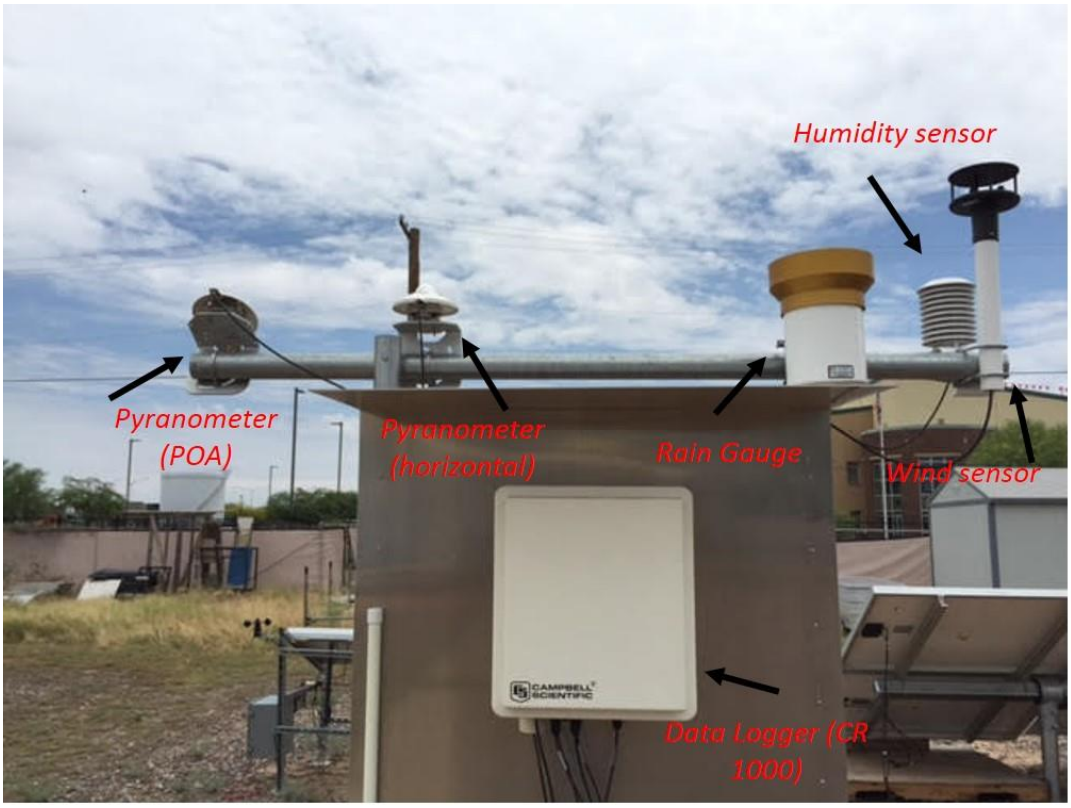

Figure 18. Weather station to measure ambient data

Open – circuit condition: In open-circuit (Voc) condition modules leads were not connected and the temperature measurement was done for three consecutive clear days. Module temperature variations is solely because of the ambient conditions and the type of insulation done on the module. Any deviation from thermal equilibrium should be because of wind speed and irradiance fluctuations.

Peak power condition: In peak power tracking (MPPT) condition, all the modules are connected to the multi-curve tracer. Module(s) power is/are continuously tracked and maintained at peak power. The temperature of the modules in this condition would depend on the ambient conditions as well as the module quality. It is well proven that

modules operate at lower temperature at MPPT than the Voc condition. This is because the heat generated by the module is dissipated continuously in the multi-curve tracer whereas at Voc condition module has to cool down by natural heat exchange with the surroundings. Figure 19 shows the modules on array connected to the multi-curve tracer.

Figure 19. Modules connected to a multitracer – Monitoring temperature at Pmax

Performance monitoring: The mutitracer is set such that it takes I-V curves of all the six modules every 5 minutes throughout the day for 2 consecutive clear sky days. These I-V curves are collected so that the module temperatures at four locations would later be correlated with these I-V parameters. These I-V curves was then be translated to STC condition based on the measured module temperature at four locations on the module. The translation procedure takes into account of the difference in temperature between the cell temperature and measured temperature on the backsheet of module. This would give a clear indication of how non-uniformity of module temperature affects the module performance prediction based on temperatures measured at different locations.

1.3.11 **Determination of module temperature coefficients**

Temperature coefficients of I-V parameters is rate of change of these parameters with respect to temperature and they determine the performance of a PV module at

various operating conditions. Temperature coefficients are measured for these modules on the array during the time of the day (around noon) when angle of incidence is close to zero. Modules are first shaded by a reflecting sheet and held at close to ambient temperature. The reflective film used had a reflectance of 94%. Modules are then connected to a multitracer and is set to take curves every 60 seconds. Now, the modules are unshaded and as the modules warm up the curves were taken. Figure 20 shows the array modules under shaded condition.

Figure 20. Modules shaded for temperature coefficient measurements

When the I-V parameters are plotted with temperature, respective temperature coefficients are calculated. Temperature coefficients are calculated with all the four temperature sensors attached to the back surface. All the temperature coefficients are plotted to see the deviation in temperature coefficients because of temperature difference between the sensors. An ideal combination of insulation configuration would be the one with less deviation in temperature coefficients.

1.4 **RESULTS AND DISCUSSION**

Results from two different phases of temperature monitoring – short-term and long-term monitoring is presented and discussed below. Initial inferences made from short-term monitoring were continued to refine the test procedure for long-term tests and there is a clear indication that insulation and electrical configuration affects temperature uniformity and module operating temperature. Results in this work is predominantly presented and discussed to analyze the effect of insulation configuration on temperature uniformity. Also, the effect of spatial temperature uniformity on measured temperature coefficients is presented.

1.4.1 **Effect of frame insulation on edge cells**

As a preliminary test, a module frame was insulated and temperature at cells close to the frame was measured and analyzed to see the effect of frame insulation on the temperature distribution. Temperature distribution of eight sensors attached to the backsheet of the module close to the edge is shown using a series of box plots in Figure 21. It is clear that when a module is frame insulated, temperature distribution on the edge cells become uniform with less deviation from median. When the frame in insulated, a warm thermal boundary is created on the edges of the module due to frame insulation. This physically reduces the convection between the ambient and the module edges and conduction between module material and the frame. Hence the only path of heat transfer is through the backsheet which tends to be more uniform, thereby reducing temperature gradients on the edge cells. This effect of thermal insulation on module boundary (frame) helps maintaining the temperature of edge cells uniform and hence between the cells in a module.

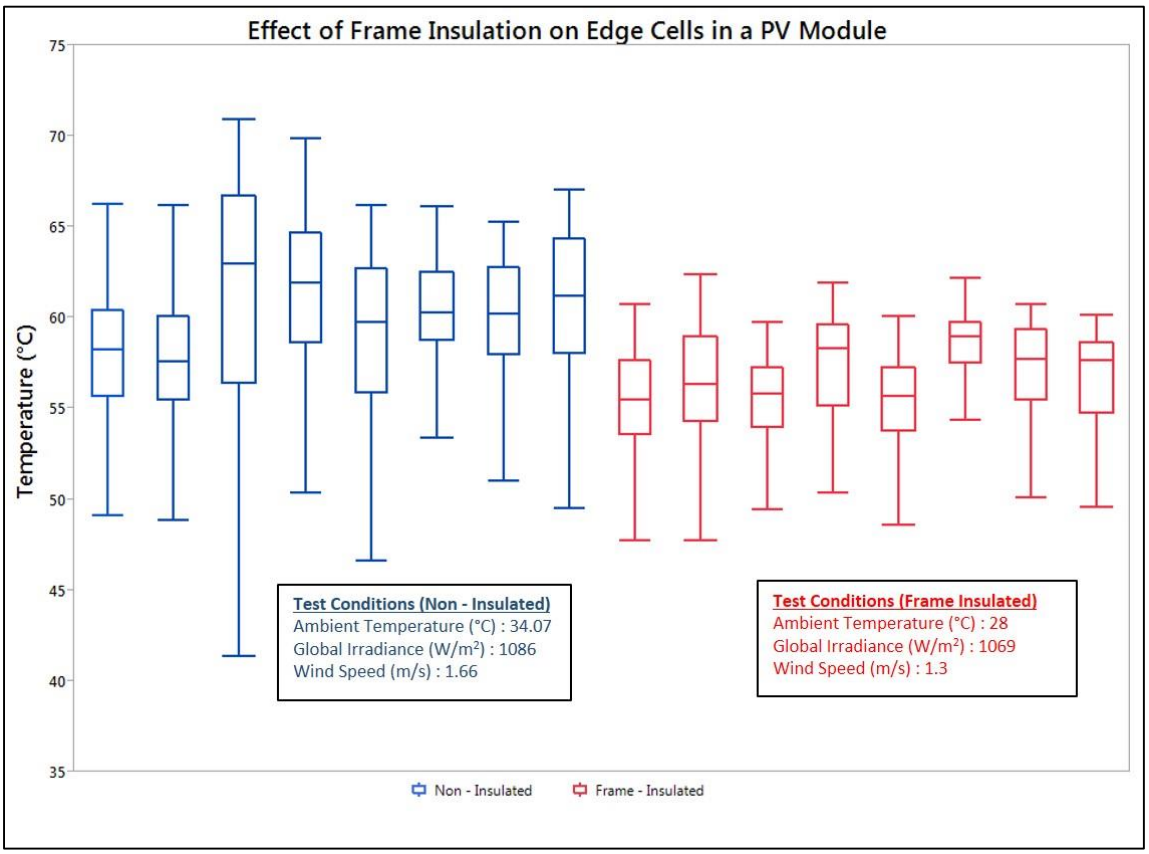

Figure 21. Effect of frame insulation on edge cells' temperature variation

When the range (difference between the quartile 1 and quartile 3) of all these plots were analyzed, it was found that for an un-insulated module it is about 7°C and for a frame insulated module it was about 2.5°C. This result proves that insulation can significantly improve temperature uniformity in a module and further work was continued based of this test result.

1.4.2 **Short-term temperature variation analysis**

As previously mentioned, the purpose of short-term monitoring is to neglect a few insulation and electrical configurations for long-term temperature tests based on obtained results and analysis from this phase of the work. Two identical modules were tested to

see the effect of insulation and electrical configurations on module temperature distribution. Temperature difference between the center cell and edge cells (average of two cells in our case) is $\Delta T_{CENTER\text{-}EDGE}$, was calculated from the data collected for 1 hour after the module was placed outdoor.

$$\Delta T_{CENTER-EDGE} = T_{CENTER} - \left(\frac{T_{LONGEDGE} + T_{SHORTEDGE}}{2}\right) \quad (3)$$

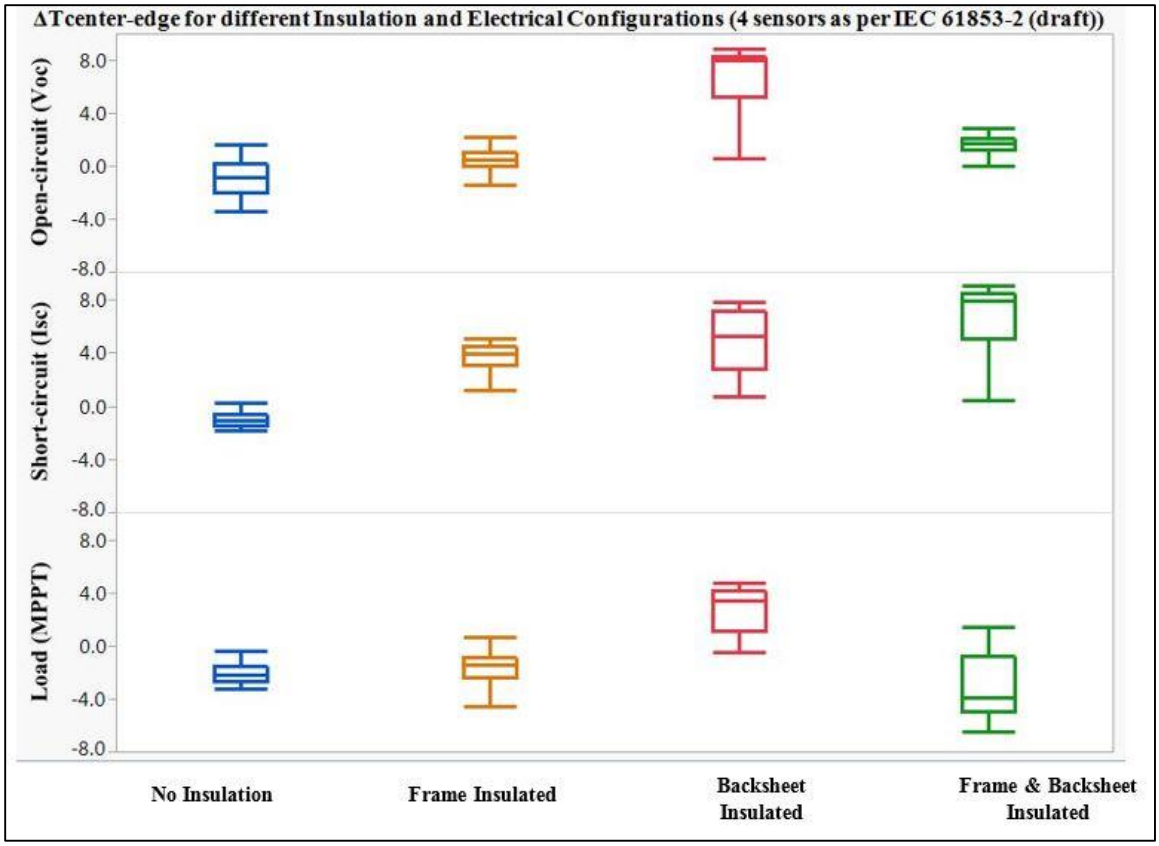

Figure 22. $\Delta T_{CENTER\text{-}EDGE}$ at various insulation and electrical configurations

At open-circuit condition (Voc), ΔT is least when a module is frame insulated and frame & backsheet insulated whereas at MPPT condition it is the least when a module in non-insulated. Module at short-circuit condition show no trend in improved temperature uniformity and this could be because of shunting in the cells above the temperature

sensor. It should also be noted that in all electrical configurations a module with 'only 'backsheet insulation has higher median ΔT and the spread in temperature difference is also higher relatively.

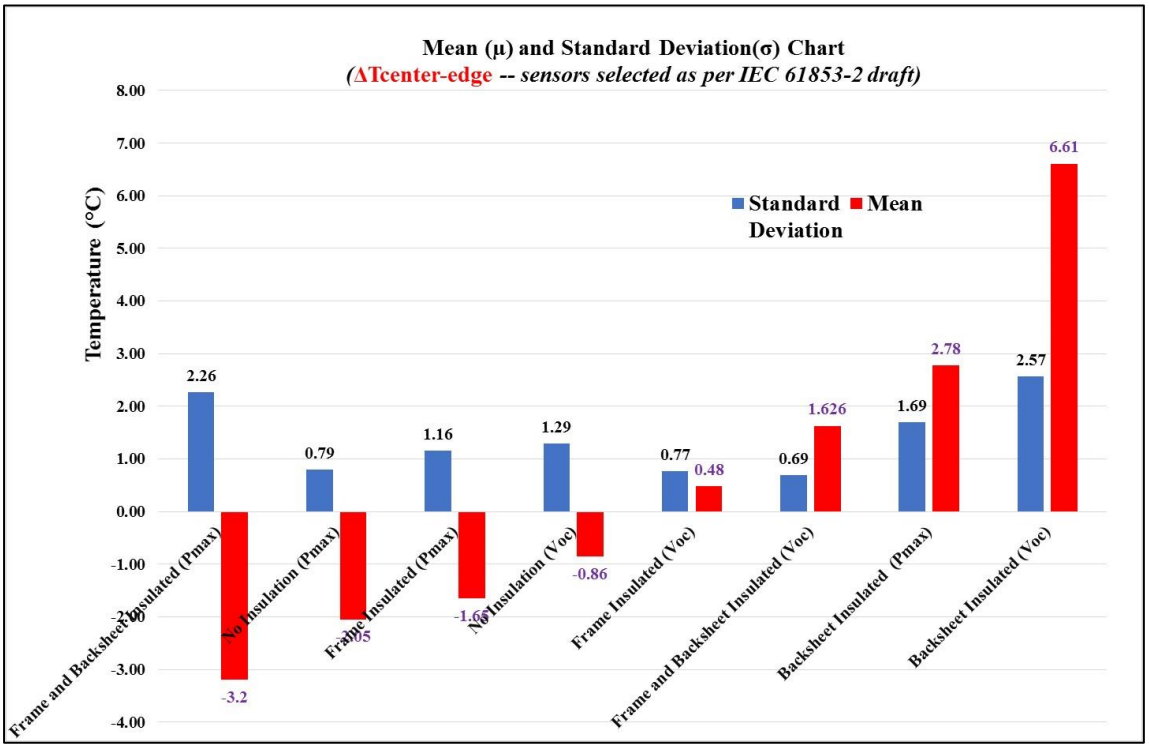

Figure 23. Mean and standard distribution chart for $\Delta T_{CENTER-EDGE}$

Mean and standard deviation of $\Delta T_{CENTER-EDGE}$ for modules at Voc and Pmax at different insulation configurations is shown in Figure 23. It is clear that the module with frame insulation at Voc has the least mean and standard deviation. In the order of least mean and standard deviation for ΔT, four ideal configurations to be considered are for long-term temperature tests are,

Frame insulation – Voc > No Insulation – Voc > Frame & backsheet insulation – Voc > Frame insulation - Pmax

As a similar analysis above, the maximum temperature difference ΔT_{MAX} between any of these four sensors was calculated and the distribution of this variation for all three electrical configurations and four insulation configurations was analyzed. Figure 24 gives the distribution of maximum temperature difference for all possible configurations and Figure 25 gives you the mean and standard deviation chart for the same.

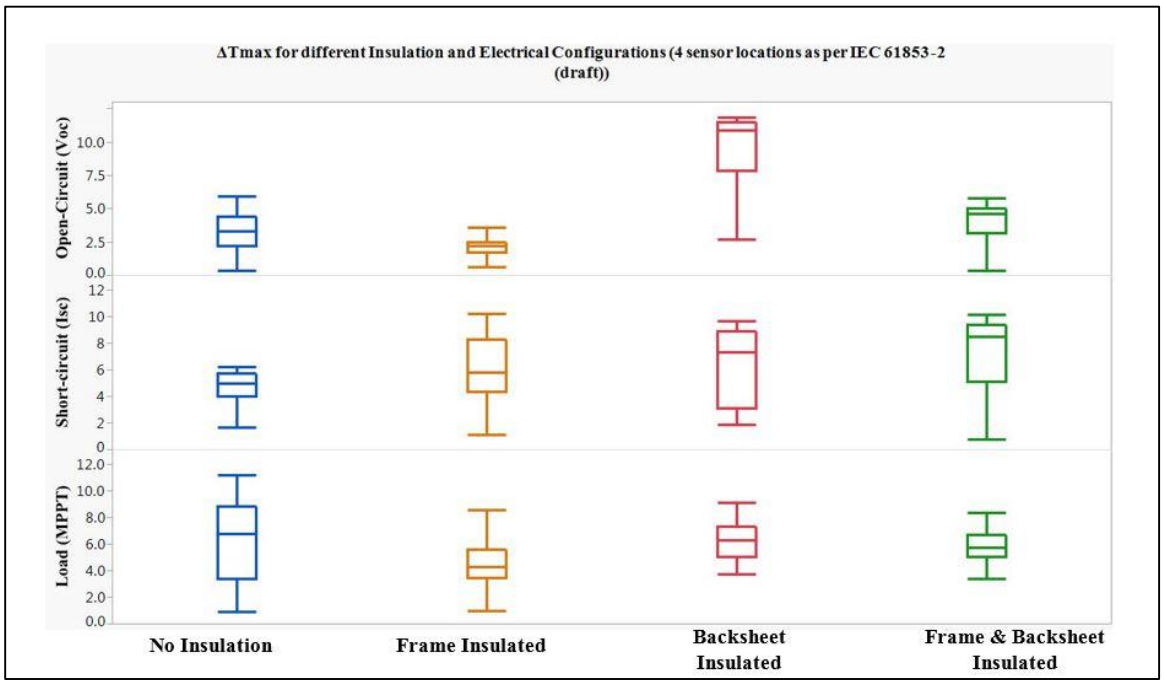

Figure 24. ΔT_{MAX} at various insulation and electrical configurations

Frame insulated module at Voc seems to have the least temperature variation among all combinations while similar to previous plots, median temperature differences are higher for Isc condition and the spread for backsheet 'only 'insulated modules seems to be high comparatively. In the order of least mean and standard deviation for ΔT, four ideal configurations to be considered are for long-term tests are,

Frame insulation – Voc > No Insulation – Voc > Frame & backsheet insulation – Voc > Frame insulation - Pmax

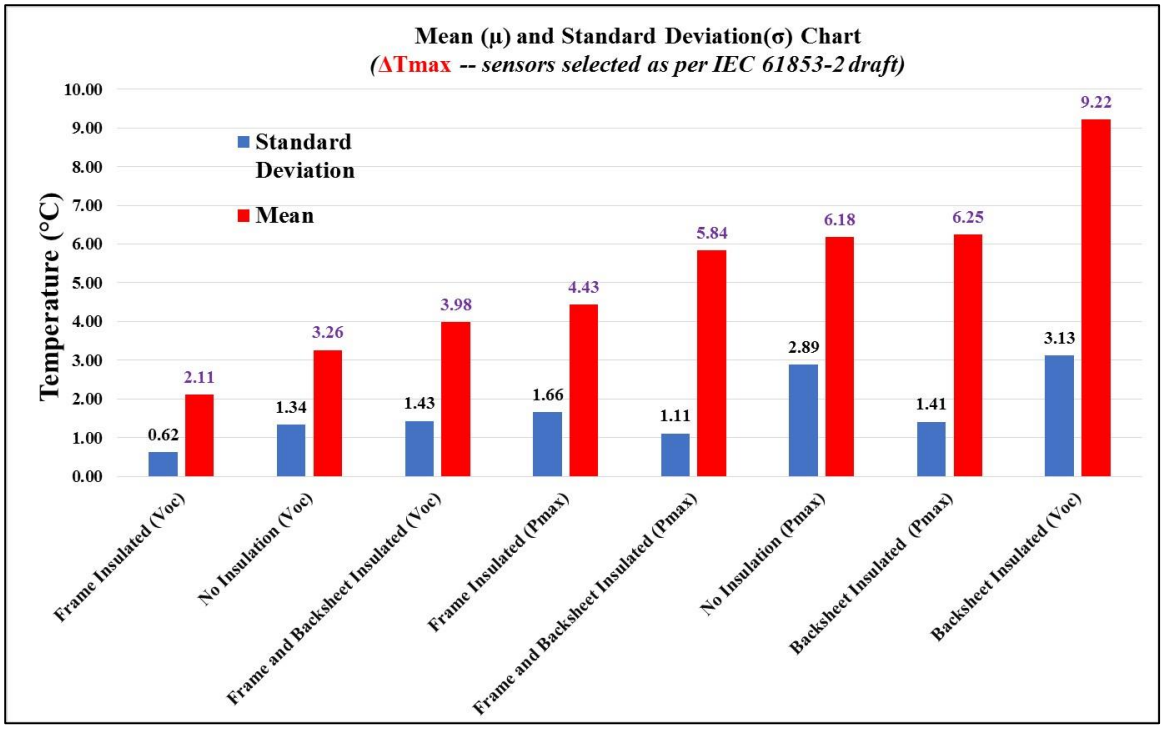

Figure 25. Mean and standard distribution chart for ΔT_{MAX}

Based on the results and analysis of temperature monitoring in these short periods few inferences are critical for the further tests and analysis.

- Spread in temperature differences are higher for ‘only ’backsheet insulated modules and this does not seem to be a good choice of insulation to improve temperature uniformity.
- Temperature monitoring at Isc seems to show erroneous trends in distribution and can be neglected. Also, modules rarely operate at short-circuit condition in the field and during actual performance testing.
- Frame insulation of modules show better temperature uniformity both in Voc and MPPT conditions.

Hence, Isc and backsheet ‘only ‘insulation will be neglected for further analysis.

1.4.3 **Long-term temperature variation analysis**

In order to more accurately predict the effect of insulation and electrical loading on temperature variability within a module long-term temperature monitoring proves to be useful to derive reliable conclusions. In this work, six identical modules were used with each module having four temperature sensors (T-type thermocouples) on their backsheet. In total, 24 temperature sensors are attached on these modules mounted on a south facing array. All the measurements were done on clear sky days to neglect the effect of irradiance changes and passing clouds on temperature variation.

1.4.3.1 **Temperature variation for modules at Voc**

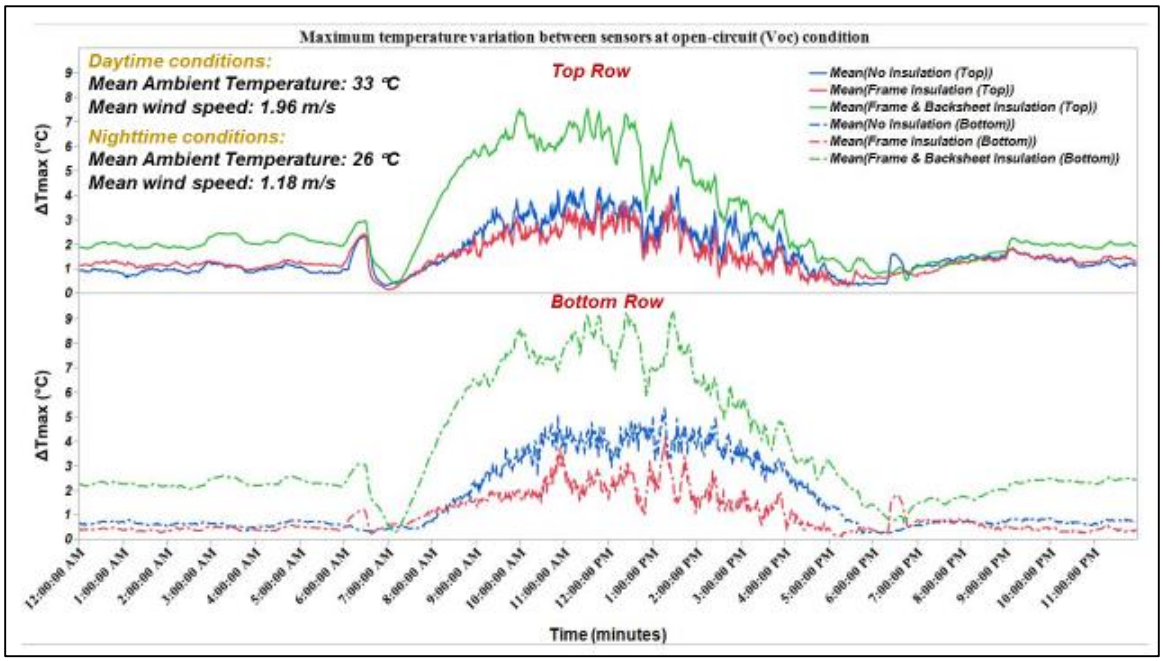

Figure 26. Time series plot for ΔT_{MAX} in array modules at Voc

The above plot is a mean time series plot for ΔT_{MAX} at Voc. The data plotted is a mean of 3 days (4.29.2015 – 5.1.2015) for all six test modules. It is clear that the frame insulated modules have least $\Delta T_{MAX.}$ It is also interesting to note that there is sudden

temperature difference during early mornings and late evenings and this is due to sudden change in irradiance on the test modules during these times most probably due to sudden solar gain in the morning and to higher angle of incidence effect with sudden solar loss caused by front glass reflection of sunlight in the evening. This is clearly illustrated in Figures A1 and A2 in APPENDIX A. Jones *et al.* [15] in their work found that the module response to irradiance change has a time lag and therefore, this peak in temperature variation is due to different cell response rates to irradiance within a module and this possibly causes instability in thermal equilibrium and higher temperature variation within a module in these times. Also, maximum temperature swings occurs when the irradiance is high during the day from 9 AM to 5PM. A time series plot showing variation in temperature during the day is shown in Figure 27. Data was filtered for irradiance > 900 W/m^2 and it clearly indicates that frame insulated module proves to improve temperature uniformity in a PV module.

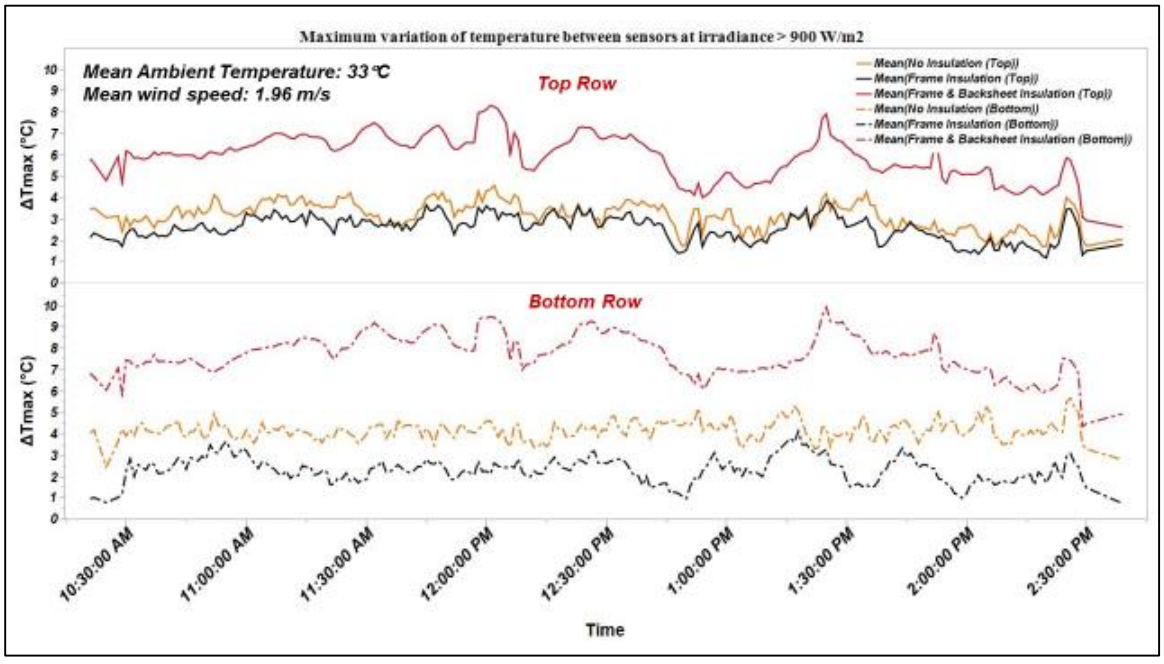

Figure 27. Time series plot for ΔT_{MAX} for POA irradiance > 900 W/m^2

A convenient way to represent temperature which has continuous variability is root mean square (RMS) and the RMS values for temperature differences was calculated for all insulation configurations. The plot below shows the trend in RMS values for different insulation configurations.

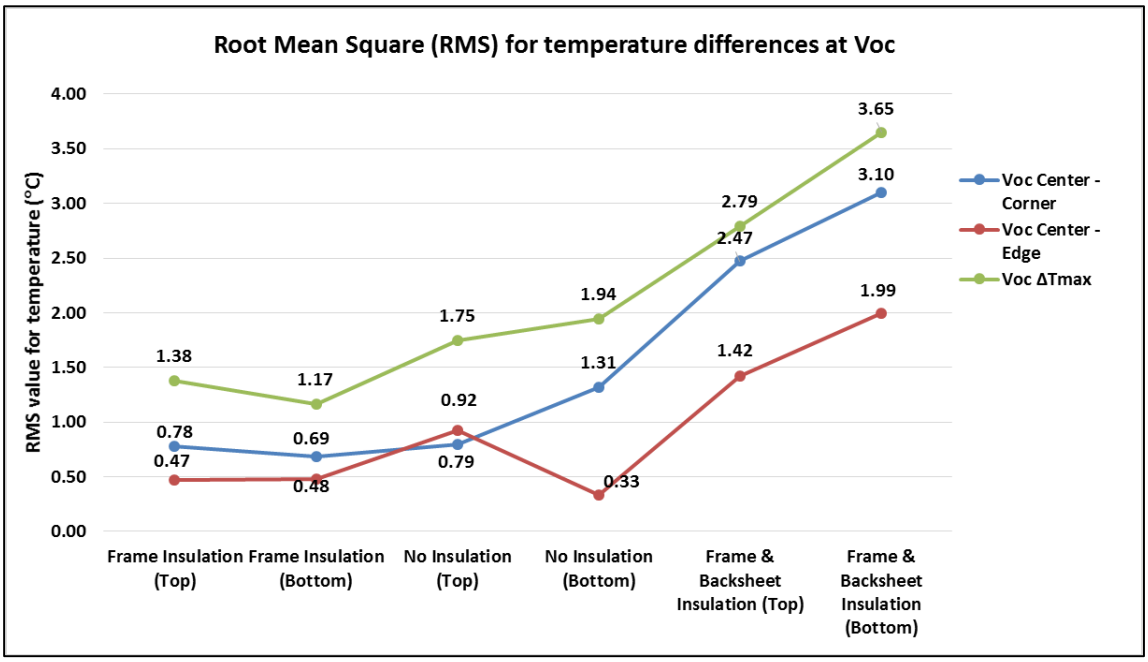

Figure 28. RMS plot for array modules at Voc

RMS values are lower for frame insulated modules which is expected because the cell-to-cell variation in temperature is considerably reduced with frame insulation. RMS values for $\Delta T_{CENTER-EDGE}$ and $\Delta T_{CENTER-CORNER}$ can be consistently less than 1°C for frame insulated modules while it increases for modules with no insulation and module with frame & backsheet insulation. Module with no insulation (top) shows irregularity in trend and this is possibly a measurement error.

1.4.3.2 **Temperature variation for modules at MPPT**

Modules usually operate at peak power condition in the field and it is very critical to analyze and measure temperature variation within a module at this condition which gives a better representation of actual cell-to-cell temperature variations within a module.

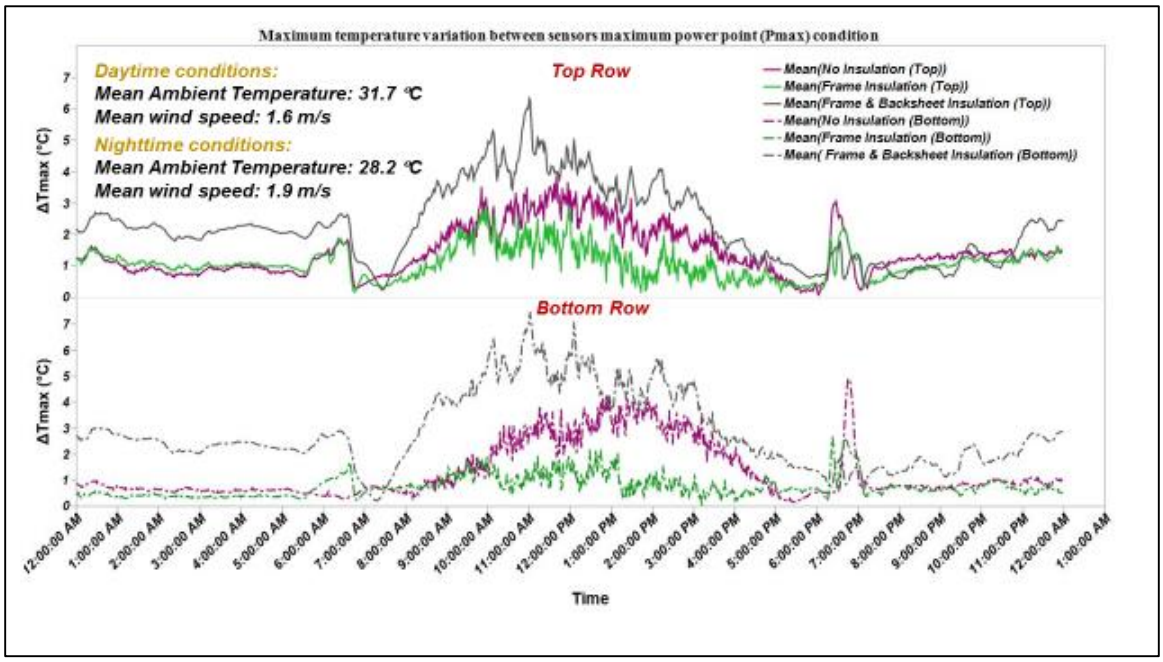

Figure 29. Time series plot for ΔT_{MAX} in array modules at MPPT

There is similar trend in temperature variation within a module at MPPT compared to Voc. Figure 29 shows a similar trend in temperature difference peaks during early morning and in evening which clearly indicates again that it is due to irradiance and irrespective of module operating condition. One could expect modules to operate at lower temperature regimes than Voc because some of the incoming irradiance is converted to electricity and is effectively dissipated when connected to load. This comparison of module operating temperature will be shown in later discussions below.

RMS values were calculated for temperature differences when they operated at MPPT and is shown in figure 30. A similar irregularity is seen in top module with no

insulation as seen in the same data point at Voc. Frame insulated modules have a consistent RMS value less than 1.5°C for ΔT_{MAX}.

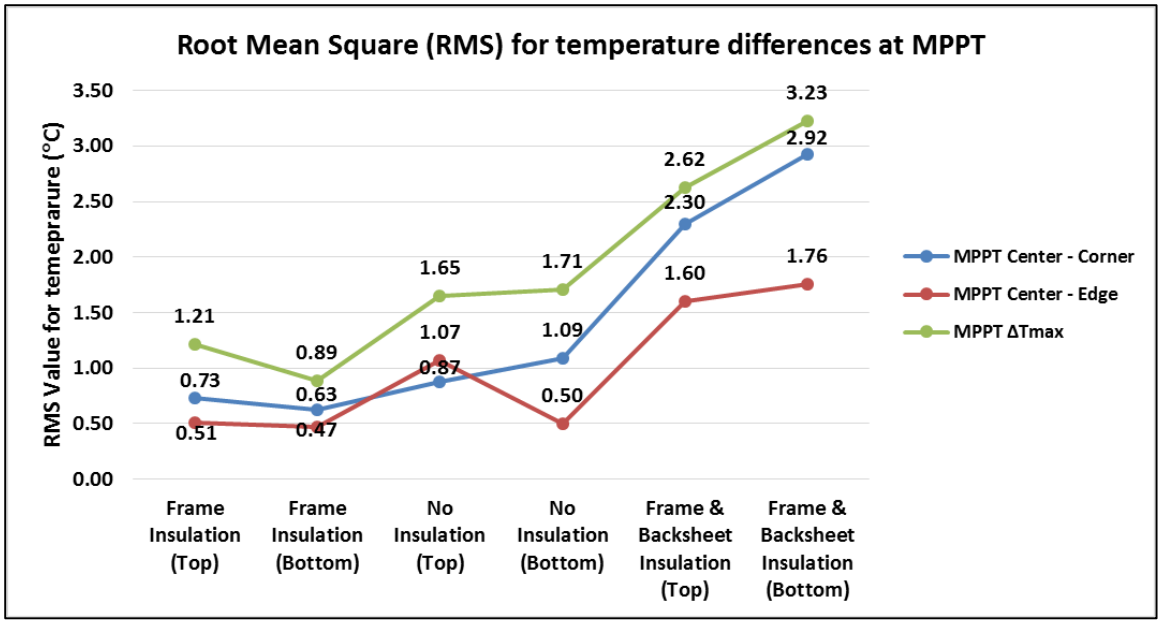

Figure 30. RMS plot for array modules at MPPT

1.4.3.3 **Comparison of Voc and MPPT**

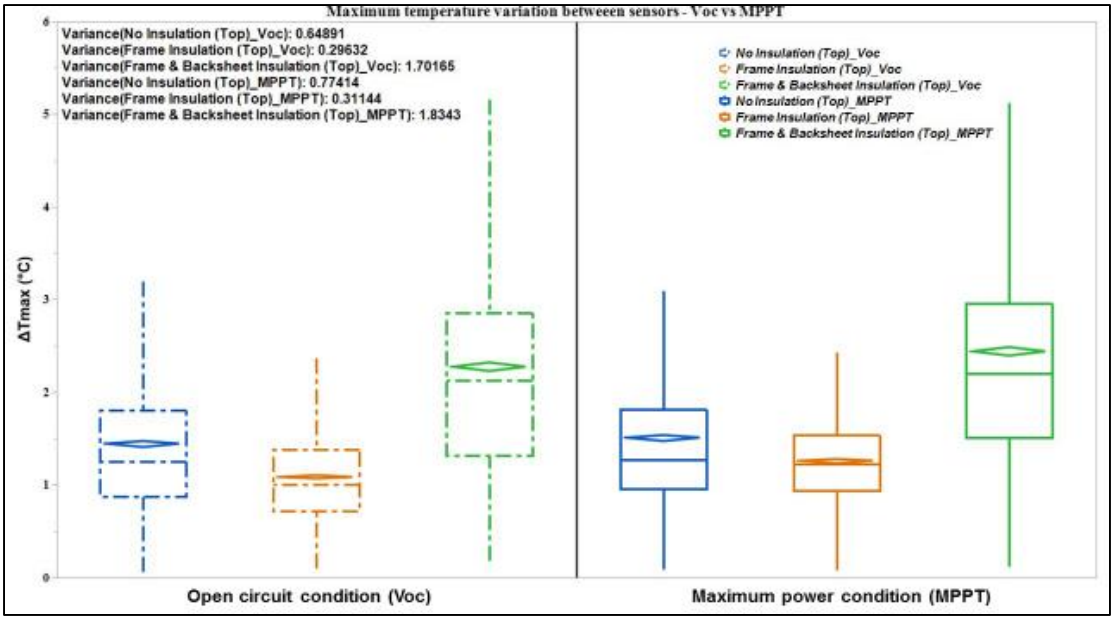

Figure 31. ΔT_{MAX} comparison for array modules at Voc and MPPT

Module electrical operating condition is one of the factors that affect the module operating temperature. Variability analysis was done to compare the effect of loading on a module and the influence of insulation on electrical configuration. It is evident from the Figure 31 that electrical configurations seems to have a less effect than insulation. When variance of the distributions are studied there is slight decrease of about 0.5°C in variance for frame insulated modules than un-insulated modules but this difference is insignificant when considering cell-cell-temperature variations.

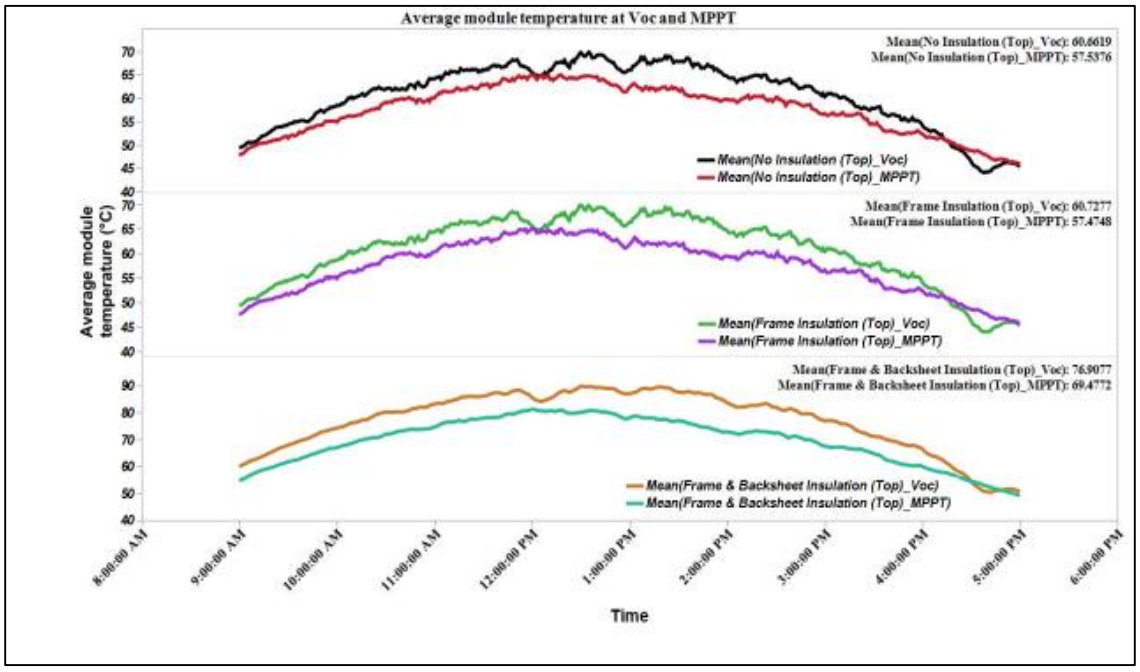

Figure 32. Comparison of module operating temperature at Voc and MPPT

Although, there is no difference in temperature variation between electrical operating conditions for the same insulation condition, modules at MPPT operate around 3°C lower than the modules at Voc. This difference in average module temperature between Voc and MPPT can go as high as 5-6°C depending on the irradiance and ambient temperature. It should be noticed that modules with frame & backsheet

insulation operate around 10 - 15°C higher than un-insulated or frame insulated modules for an obvious reason that heat transfer from the back surface and the frame is restricted and the only surface the heat can be dissipated in this case is through the front glass surface of the module.

1.4.4 **Performance variation due to module temperature non-uniformity**

Temperature variation within a module is highly significant that it can affect the prediction of module performance to a considerably. During the experiments in this work, all the test modules were continuously monitored for performance and temperature for two clear sky days at MPPT condition. All these I-V curve data was then translated to Standard test conditions (STC) using the measured irradiance, ambient temperature and most importantly four module temperatures at various locations within a module. All the curves were translated separately using each of the four temperatures to see the difference in performance parameters due to change in measure module temperature.

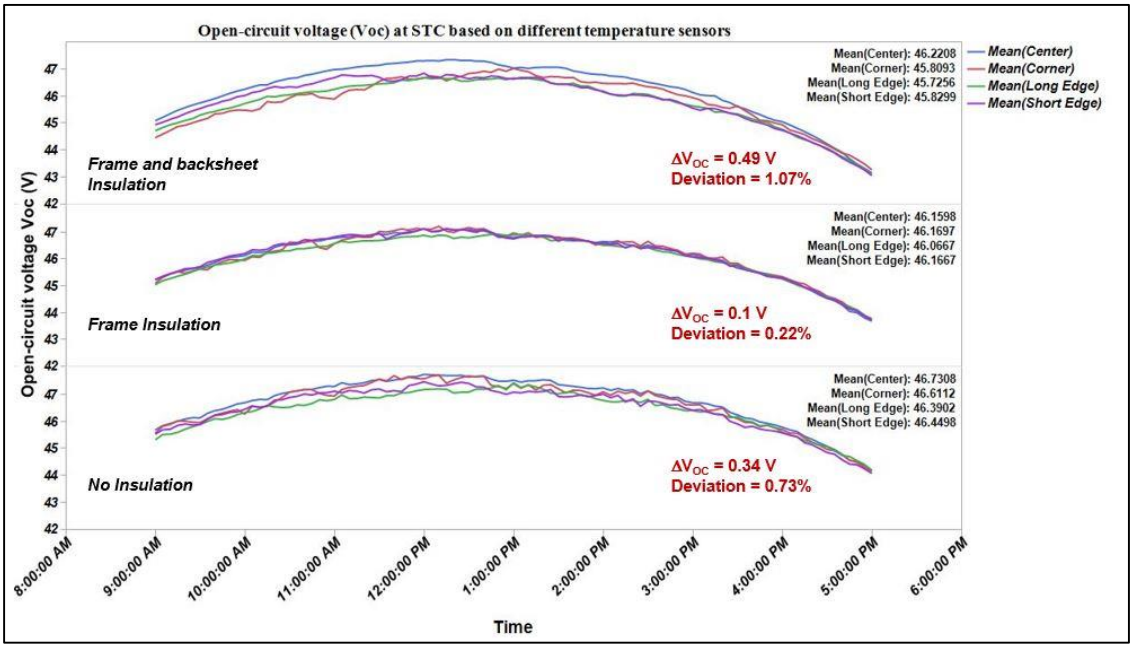

Figure 33. STC Voc vs module temperatures for various insulation configurations

Figure 33 shows STC translated Voc measured during day 9 AM – 5 PM using four temperature data sets. When a module is frame insulated, the difference in mean STC Voc can be about 0.1 V, while the module is not insulated it can be 0.34 V and when frame & backsheet insulated it can be 0.49 V. A similar plot is given below for power and the effect of temperature variation is more prominent in power than in voltage due to a combined effect of voltage and fill factor differences on power.

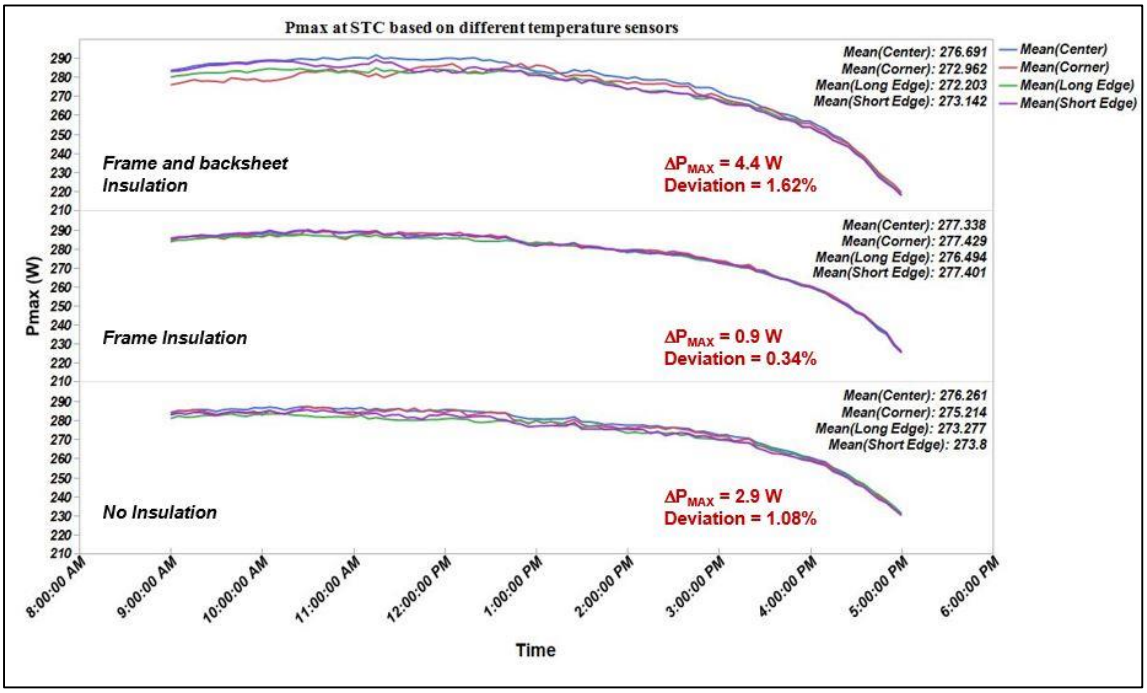

Figure 34. STC Pmax vs module temperatures for various insulation configurations

For an un-insulated module the mean difference in power can be about 2.9 W whereas for a frame insulated module it can be reduced to 0.9 W. This difference in Pmax and Voc can be higher during the maximum power generating periods – during day which can be clearly seen in the plots above. The implications of these voltage and power differences is very severe when it comes to rating a module and accuracy of string level MPPTs in the power plants.

RMS values for these voltage and power differences are calculated for each insulation configuration. It is interesting to note that they have a similar trend for both voltage and power but the impact on power is relatively significant than voltage. It is clearly seen that an RMS value for Voc and Vmp of about just 1 V can lead to a RMS value of 9 W in power which is significant when it comes to module power rating.

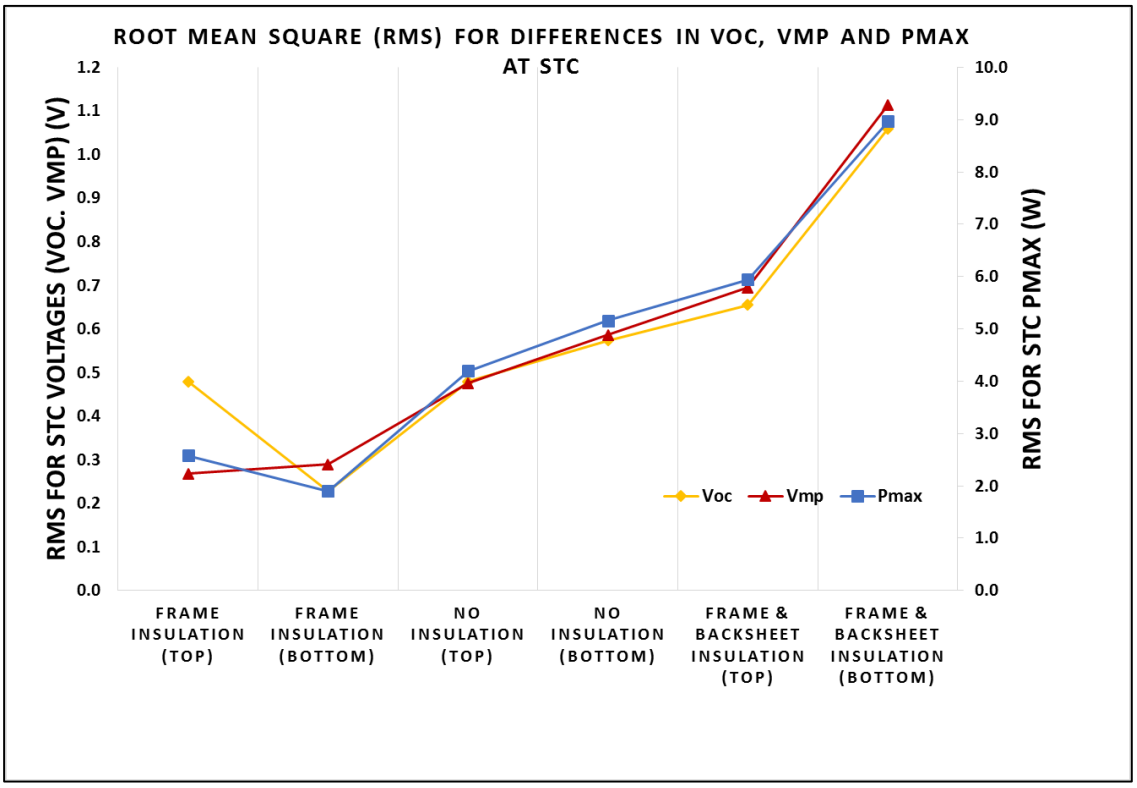

Figure 35. RMS plot for STC voltages and power for different insulation configurations

Thereby, in order to accurately report the operating temperature during module power rating at STC, the module under test should be frame insulated and use a single thermocouple (since the temperature variations are less) or use the average of four thermocouple temperatures as specified in IEC 61853-2 without any insulation to account for all possible spatial temperature variations within a module.

Table 3

RMS voltage and power differences at STC

Insulation configuration	Row	Voc (V)	Vmp (V)	Pmax (W)
Frame Insulation	Top	0.48	0.27	2.58
Frame Insulation	Bottom	0.23	0.29	1.90
No Insulation	Top	0.48	0.48	4.19
No Insulation	Bottom	0.57	0.59	5.16
Frame & Backsheet Insulation	Top	0.66	0.69	5.95
Frame & Backsheet Insulation	Bottom	1.06	1.11	8.97

1.4.5 **Influence on module temperature coefficients**

Temperature coefficients measurements can also be significantly affected by these temperature variations within a module. Results from baseline testing of array modules proves how insulating the module frame can drastically reduce the inaccuracy in temperature coefficients measurement.

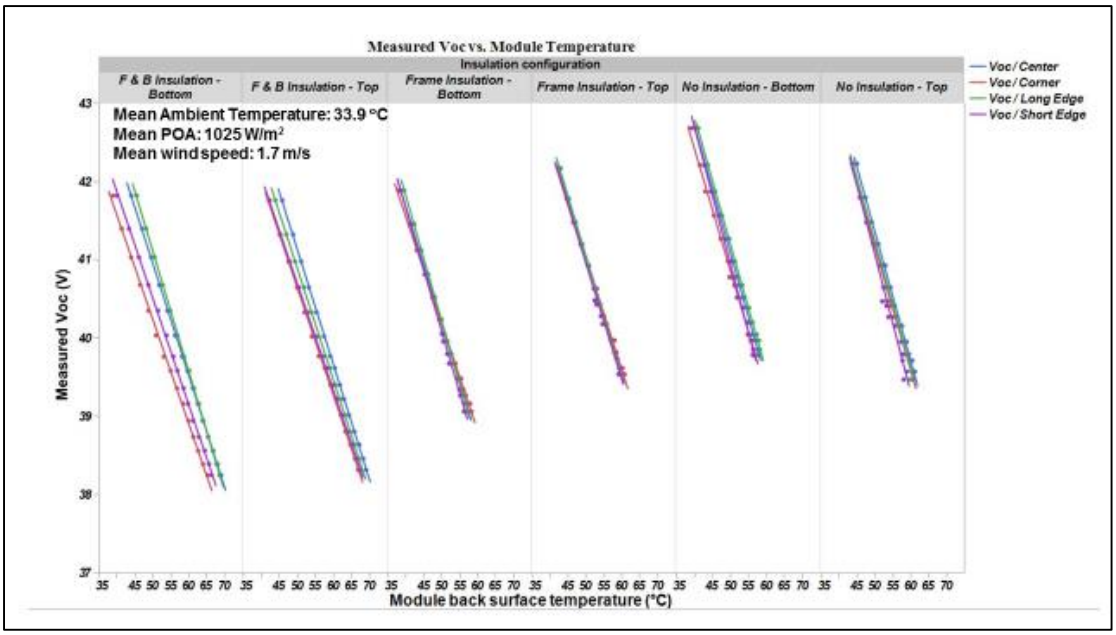

Figure 36. Voc temperature coefficients at different insulation configurations

Since, temperature directly affects voltage and power more than current, it is important to analyze and discuss the effect of temperature differences on these coefficients.

Temperature coefficients for Voc, ($\frac{dVoc}{dT}$), obtained by four different temperatures for each module are compared to see their deviation from each other and it is clear from the above plot that frame insulated module has a higher accuracy followed by un-insulated module and then the frame & backsheet insulated module. Temperature distribution of all modules during the baseline test is shown in APPENDIX A.

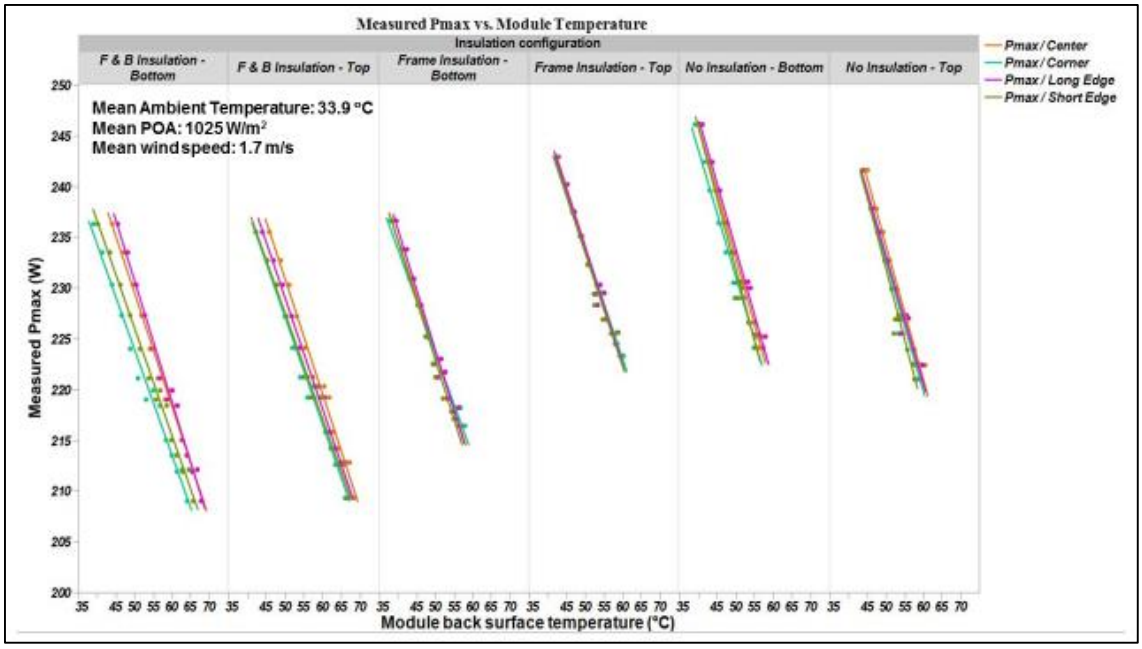

Figure 37. Pmax temperature coefficients at different insulation configurations

Temperature coefficient for Pmax, ($\frac{dPmax}{dT}$), is also derived based on different insulation configurations and location of temperature sensors. Cell-to-cell differences in temperature leads to higher inaccuracy in Pmax temperature coefficient measurement than Voc. It is very clear from the Figure 37 that the Pmax temperature coefficient has

lowest deviation for modules with frame insulation. Temperature coefficient values for all the I-V parameters are given in APPENDIX A.

Deviation in temperature coefficients: Percentage change in individual temperature coefficients from the average is calculated as shown below.

$$Total\ \%Change = \frac{(\%Change_{center} + \%Change_{corner} + \%Change_{longedge} + \%Change_{shortedge})}{4} \quad (4)$$

$$\%\ Change_{center} = \frac{TC_{center} - average(TC_{center} + TC_{corner} + TC_{longedge} + TC_{shortedge})}{average(TC_{center} + TC_{corner} + TC_{longedge} + TC_{shortedge})} \times 100 \quad (5)$$

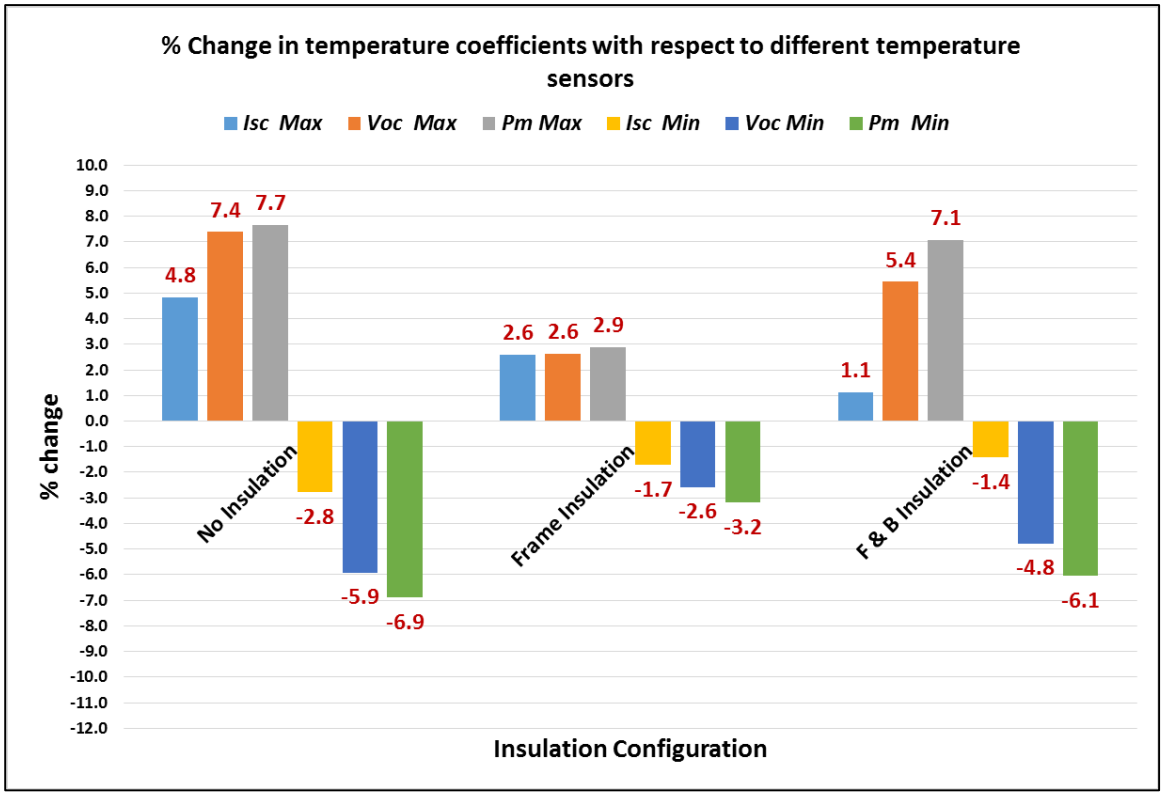

Figure 38. Deviation in temperature coefficients based on temperature differences

Frame insulated modules have less deviation in temperature coefficients within ±3% where in un-insulated modules and frame & backsheet insulated modules this deviation can go as high as ±7% in temperature coefficients which is significant for performance testing and rating a module.

1.5 **CONCLUSION**

In this first part of the thesis, the influence of spatial temperature distribution on the accuracy of performance data of photovoltaic (PV) modules in outdoor conditions is extensively studied under different thermal insulation conditions so an accurate performance data can be obtained during the field measurements. This study clearly indicates that there is a large spatial temperature difference between various thermocouple locations specified in IEC 61853-2 (cells at the center, corner, near long frame and near short frame). This investigation concludes that the best temperature uniformity and the most accurate I-V data can be obtained only by thermally insulating the inner and outer frame surfaces or by using the average of four thermocouple temperatures, specified in IEC 61853-2, without any thermal insulation.

Based on temperature monitoring of modules at different configurations, the following additional or specific conclusions can be obtained.

- In any given uninsulated module, one should expect a maximum cell-to-cell temperature variation of about 2 – 4 °C depending on the ambient conditions.
- Frame insulation of a PV module can considerably improve spatial temperature uniformity within a module and thereby improving the accuracy of power rating of a module irrespective of the location of the temperature sensor. If practical in the field, the frame-insulated method is the most accurate and recommended method to determine the performance of the module.
- For uninsulated modules, reporting the performance data based on the average temperature for thermal sensors, as specified in IEC 61853-2 standard, is the second most accurate and recommended method during the field measurements.

- In addition to power rating measurements, the measurement of temperature coefficients of a module under real outdoor conditions is very important and even small temperature gradients within the module can lead to as high as ±7.7% variation in temperature coefficients for the uninsulated modules. This variation can be reduced to ±3% if the module frame is insulated. Therefore, for the measurement of temperature coefficients, the best method is the frame insulated method.
- Overall, the following conclusions can be made: Obtain the outdoor I-V curves for all the test modules using the frame insulated method with one or four temperature sensors (best method) or using the uninsulated method with four temperature sensors (second best method); obtain the outdoor temperature coefficients just for one or a few representative modules using the frame insulated method with one or four temperature sensors.
- Modules at MPPT operate around 3°C less than modules at Voc and this can increase to as high as 5 - 6°C when irradiance and ambient temperature are higher.
- Based on continuous and simultaneous performance and temperature monitoring investigation in this study over a long period, it is clearly shown that the cell-cell temperature variation can lead to significantly inaccurate performance measurement data depending on the location of the temperature sensor in a module.

PART 2: STATISTICAL DETERMINATION OF DOMINANT DEGRADATION MODES IN PV MODULES

2.1 INTRODUCTION

2.1.1 Background

PV Modules degrade in field condition due to design quality, manufacturing issues and most importantly field environmental conditions. One or multiple degradation modes would cause degradation of one or more of I-V parameters (Isc, Voc, FF) leading to power loss in a module. I-V parameters degrade due to one or more degradation modes that is visible as physical changes in cell, encapsulant, metallization, substrate, superstrate and more.

Understanding power degradation rate is important from manufacturers' perspective to improve the design quality of a photovoltaic (PV) module, whereas understanding the same is important from the perspective of plant owners and investors to evaluate the present worth of the plant. This can only be done by predicting degradation rates and understanding the reliability of PV modules with respect to degradation modes and mechanisms, module design and environmental conditions [16]. This study is aimed at correlating performance degradation of field aged modules with field visual defects or degradation modes to understand the degradation modes that affect the module performance. By understanding this correlation, the researchers could focus their material characterization and analysis to identify the degradation mechanism(s) responsible for the degradation modes, and thereby improve module design and packaging.

2.1.2 **Scope of the work**

Scope of this work includes,

- Calculating degradation rates of power and other I-V parameters using measured I-V curve data.
- Using statistical methods to correlate I-V parameters with power and identify the I-V parameter that is most affected.
- Mapping the visual defects data with performance data to identify the dominant defect affecting power degradation in two different climatic conditions.

2.2 **LITERATURE REVIEW**

Reliability and durability of PV modules is critical to understand module performance and failures involved. If the module power drops beyond a specified limit and is replaced/removed from the field then it is a reliability failure. Reliability failures occur mostly due to the design and production issues, and eligible for the warranty claims [17]. If the performance of PV modules degrades, but still meet the warranty requirements then they are called durability failures. Durability issues could be attributed due to the materials or material systems used for manufacturing the PV modules. In general, PV modules degrade/fail due to multiple failure modes which are caused due to multiple failure mechanisms.

Usually, the lifetime of PV modules is typically dictated by the degradation rates rather than failure rates. However, multiple failure modes over time could have cumulative influence on the degradation rates of the PV modules. However, determining failure rate is complex and it depends on various factors such as location of the module installed, climatic conditions, duration of the module in the field, type of modules etc., An extensive study on failure and degradation modes of PV modules in hot-dry climate was reported in a previous study done by ASU–PRL and it is reported that the major causes for power degradation in glass/polymer modules fielded in hot–dry climate are fill factor (FF) and short circuit current (Isc) [18, 19]. Chattopadhyay *et al.* [20] have identified that encapsulant discoloration and corrosion are primary degradation modes based on their study on modules installed in different climatic locations in India. Another work at ASU–PRL statistically analyzed the performance parameters to identify the I-V parameter (Isc, Voc or FF) that affects the power drop [21].

Statistical techniques: In order to understand the methods used for this analysis few terms need to be defined and are given below.

Pearson Correlation: It is statistical test to determine the linear correlation between data sets to see how well they are related. The value of this statistical test range from -1 to +1, where +1 means if one parameter increases other parameter increases and -1 means they are opposite and 0 means no dependence.

Hypothesis Testing: Hypothesis testing is a test for statistical significance between two samples in a population. In this method, we test our claim/hypothesis by determining the probability that a sample statistic (variable) could have been selected if the hypothesis were true.

Null and Alternate Hypothesis: Null hypothesis usually denoted by Ho is a statement about a parameter that is assumed to be true. It is usually the opposite of a statement you would want to prove. Alternate hypothesis usually denoted by H1 is a statement contradictory to null hypothesis where the parameter is either less than, greater than or not equal to the value stated. It is usually the statement you would want to prove.

This work employs statistical tools such as Pearson correlation and hypothesis testing to identify the most affected I-V parameters responsible for power degradation. This work also correlates field visual defects data that is obtained using our extensive visual inspection study with the affected performance parameters to identify the dominant degradation modes or defects influencing power drop.

2.3 **METHODOLOGY**

2.3.1 **Data collection**

Performance degradation of each power plant was determined through field testing by collecting I-V curves of individual modules in the best, median and worst strings of the whole plant. These strings were selected statistically based on the performance of the string as a whole and then all the modules were tested individually in these selected strings. All field data were collected under acceptable prevailing conditions. These collected data were then translated to standard test conditions - STC (25°C, 1000W/m^2). Figure 39 shows an overall flowchart of power plant evaluation procedure followed by ASU-PRL.

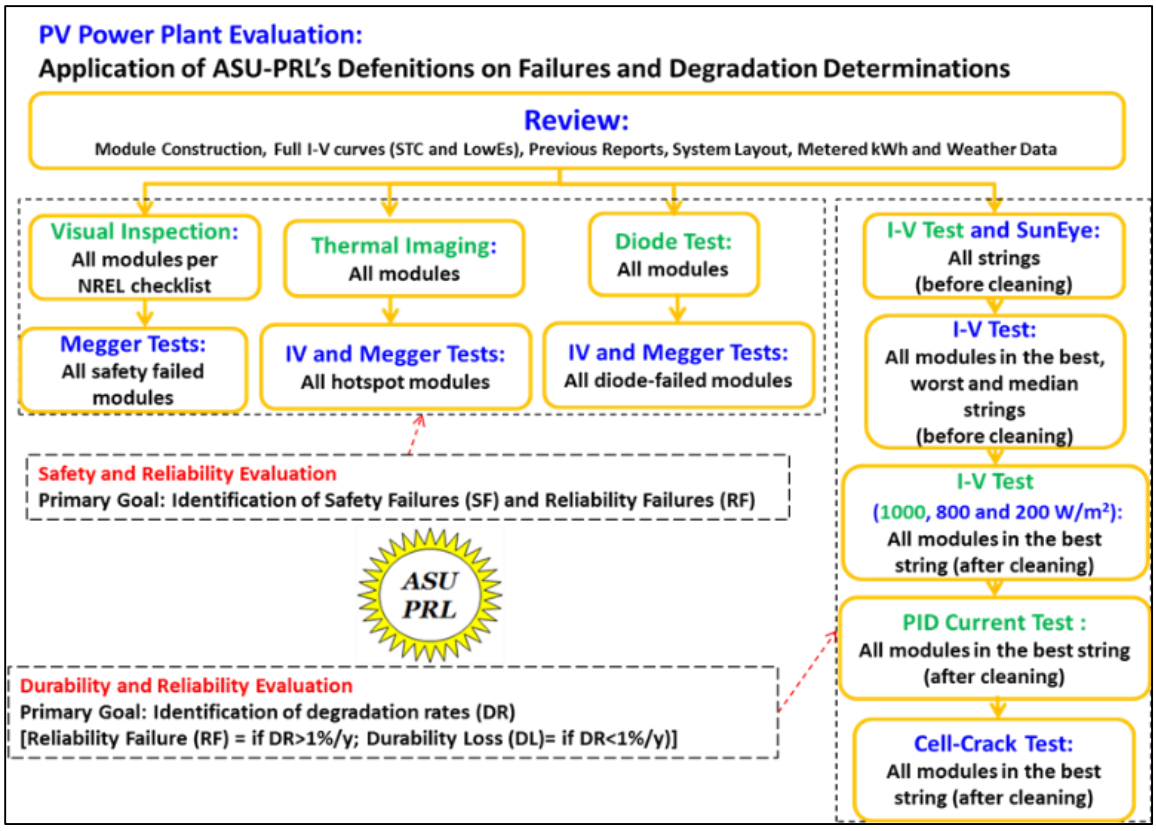

Figure 39. ASU – PRL Power plant Evaluation Procedure

Visual Inspection data of these modules were obtained using visual inspection checklist modified by ASU-PRL based on the one developed by NREL [22]. Characterization tools such as IR camera and diode checker were also used to identify failures that cannot be investigated by human eye. Table 4 provides the specifications of the systems considered for this analysis.

Table 4
System and module specifications

System	Model G	Model HP	Model CT	Model J	Model JVA
Mounting	Ground mount	Roof mount	Roof mount	Roof mount	Roof mount
Module Technology	Mono-Si	Mono-Si/a-Si (HIT)	Poly-Si	Poly-Si	Poly-Si
Construction	G/P/FL	G/P/FR	G/G/FR	G/P/FL	G/P/FR
Location	Glendale (AZ)	Scottsdale (AZ)	Tempe (AZ)	Yonkers (NY)	Valhalla (NY)
Climate	Hot-dry	Hot-dry	Hot -dry	Cold-dry	Cold-dry
Years Fielded	12	5	9	18	19
Number of modules evaluated	285	78	115	45	124

Visual defects of these modules are then correlated with the module performance parameters obtained from the I-V curves collected for individual modules to identify the most dominant degradation mode causing power degradation in the modules. Figure 40 shows the defect count of all 647 modules that are considered for evaluation from all the 5 power plants. Individual plant defects chart for all the models are given in APPENDIX B. Majority of the modules had multiple defects which might have accelerated the severity of each other, eventually leading to module performance losses.

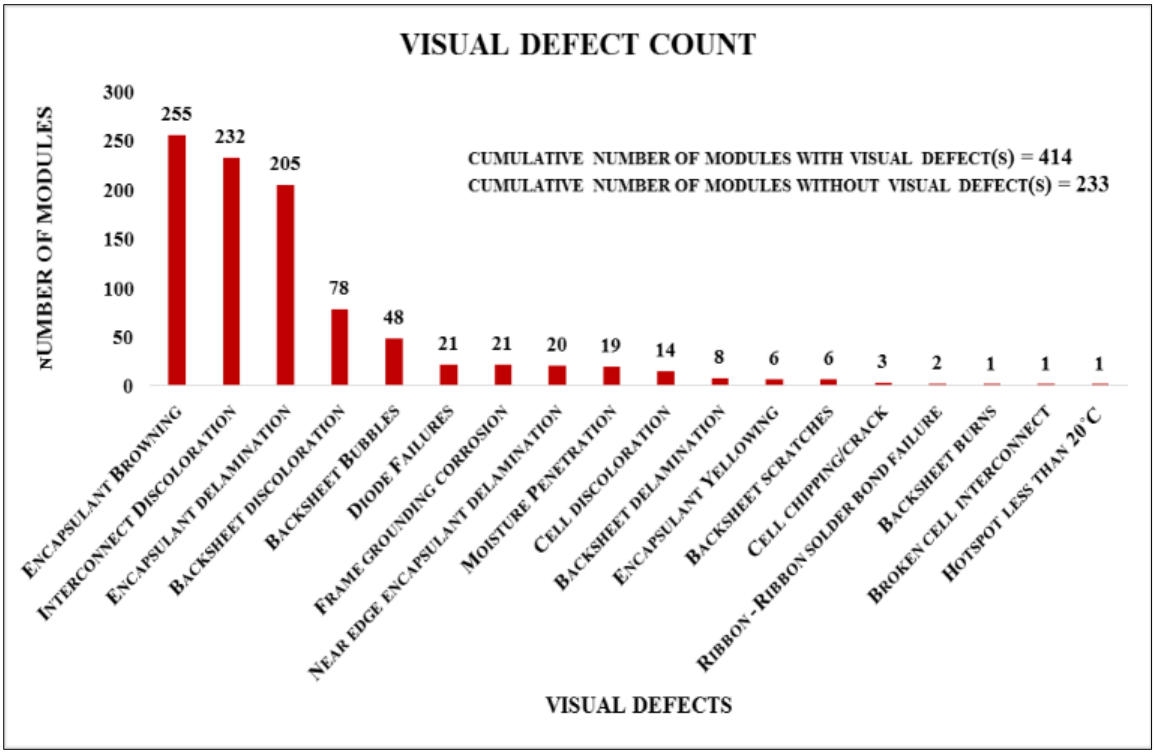

Figure 40. Visual defects of 647 modules in five power plants

2.3.2 **Analysis procedure**

As a primary step in our analysis the degradation rates of the performance parameters (Isc, Voc, FF, Rs, Rsh) were calculated assuming linear degradation for all the parameters in crystalline silicon modules. To identify the most influential defect on power drop, two statistical methods, Pearson correlation and hypothesis testing, were performed on the degradation rates of the performance parameters. Once these tests are done, the statistical order of influence is identified and then the defects are correlated with degradation rates of performance parameters.

MINITAB, a statistical software, was used to perform the analyses. Pearson correlation test is done on the degradation rates to estimate the linear relationships between the degradation rates of the performance parameters. Equal variance is assumed

because the measurements was done with the same instruments and the data is all translated to STC conditions. A similar test was performed between series resistance, shunt resistance, and fill factor to see their correlation.

In order to determine the parameter that is influencing the power degradation in a module, a statistical technique called hypothesis testing is performed on the degradation rates of the performance parameters. This test of significance has two hypothesis statements, namely null and alternate hypothesis. The null hypothesis can be stated as H_o: $\mu_o = \mu_1$ where μ_o and μ_1 are means of two different parameters in consideration. The alternate hypothesis can be stated as $\mu_o < \mu_1$ or $\mu_o > \mu_1$ or $\mu_o \neq \mu_1$, in our case it was set as $\mu_o < \mu_1$. The degradation rates of all the parameters are populated in a worksheet. The significance level of the test is set as 0.05. The parameter to be noted from a hypothesis test result is a p-value, which is the probability of occurrence of the given statement. When the p–value is less than that of the significance level then we reject null hypothesis. This procedure is followed for all possible combinations of performance parameters and the most significant parameter affecting power drop is found. Now, the visual defects and the performance parameters are plotted to see the defect that is more correlating with the factor that is affected the most, thereby determining the dominant degradation mode.

2.4 **RESULTS AND DISCUSSION**

2.4.1 **Power Degradation**

The field data of module performance was analyzed to calculate the annual degradation rate of the plant, assuming they degrade linearly. Figure 41 shows the distribution of power degradation rates of sampled modules in all five plants.

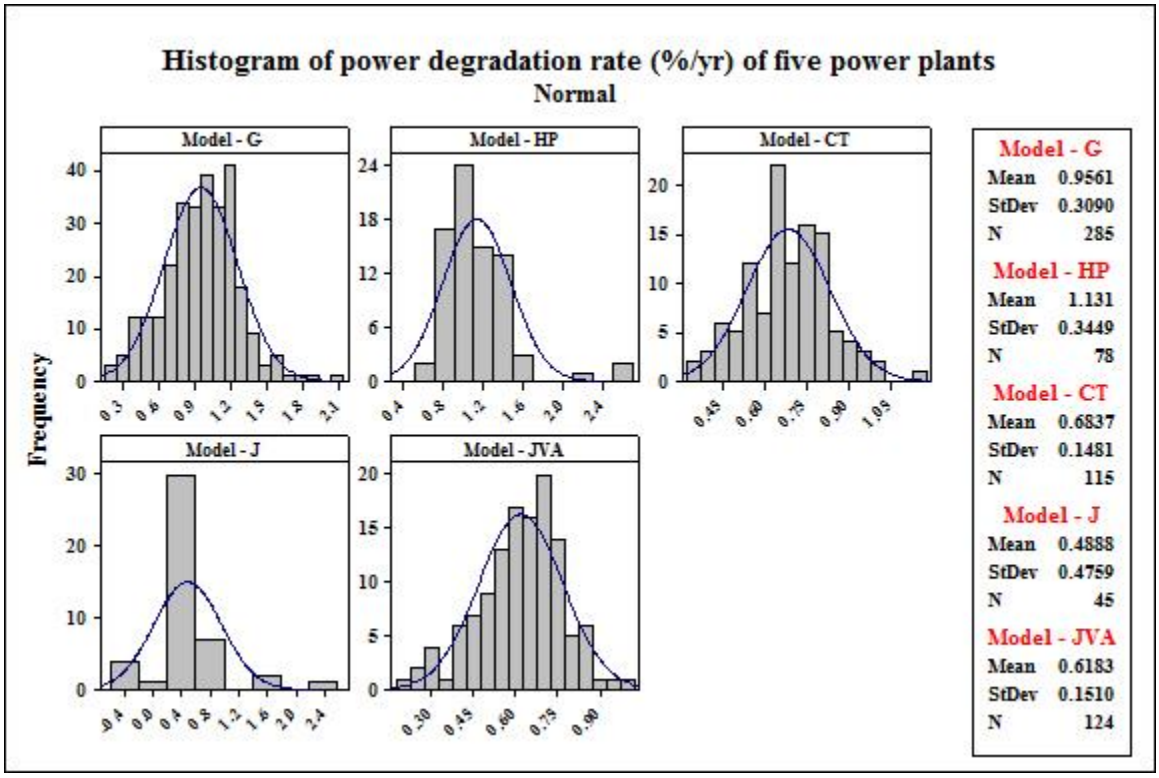

Figure 41. Histogram of power degradation for all power plants (%/year)

Individual degradation rates for Pmax (%/year) is plotted in figure 42 and it can be clearly seen that modules in cold dry climate even after 18 and 19 years of field age have comparatively less degradation rates than plants in hot-dry climate. The values given are median degradation rates (%/year).

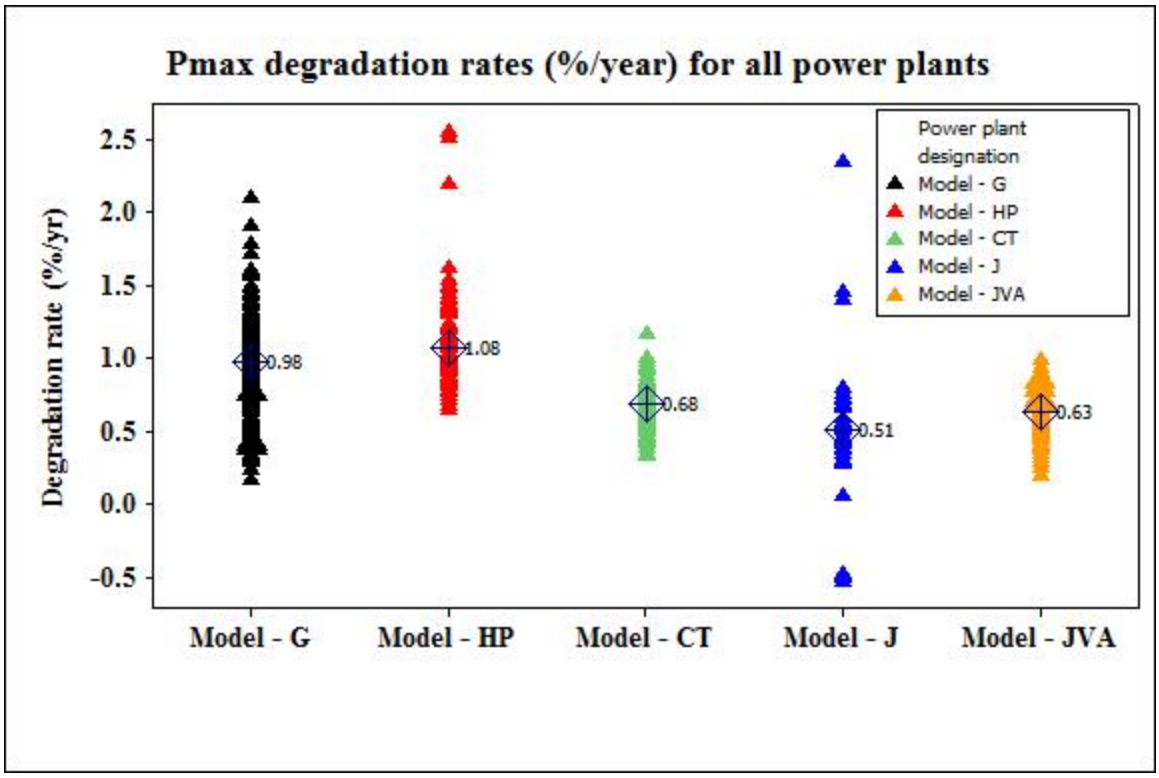

Figure 42. Comparison of power degradation rate for all power plants (%/year)

Table 5

Mean and median degradation rates for modules in five plants

MODEL	Mean degradation rate (%/year)	Median degradation rate (%/year)
Model - G	0.95	0.96
Model - HP	1.13	0.91
Model – CT	0.68	0.68
Model - J	0.49	0.51
Model – JVA	0.61	0.63

2.4.2 **Correlation between Pmax and I-V Parameter Degradation**

Correlation tests such as Pearson correlation and hypothesis testing (2 – sample t-test) was performed in MINITAB and the relationships between the I-V parameters were identified to analyze the most affected I-V parameter in a power plant. It also helps in determining the order of statistical significance among these parameters. These analyses are based of the degradation rates of I-V parameters for individual modules.

2.4.2.1 **Pearson Correlation**

Based on the correlation test on the performance parameters, it was identified that the FF is more correlated to Pmax for modules in hot-dry climate, whereas Isc is more correlated for modules in cold-dry climate. Figures 43 to 47 show the box plots of Isc, Voc, FF, and Pmax degradation rates for all five power plants. Series resistance increases primarily due to metallization and/or solder bond issues and shunt resistance losses is primarily due to manufacturing issues. Rsh issue becomes significant at low irradiance levels.

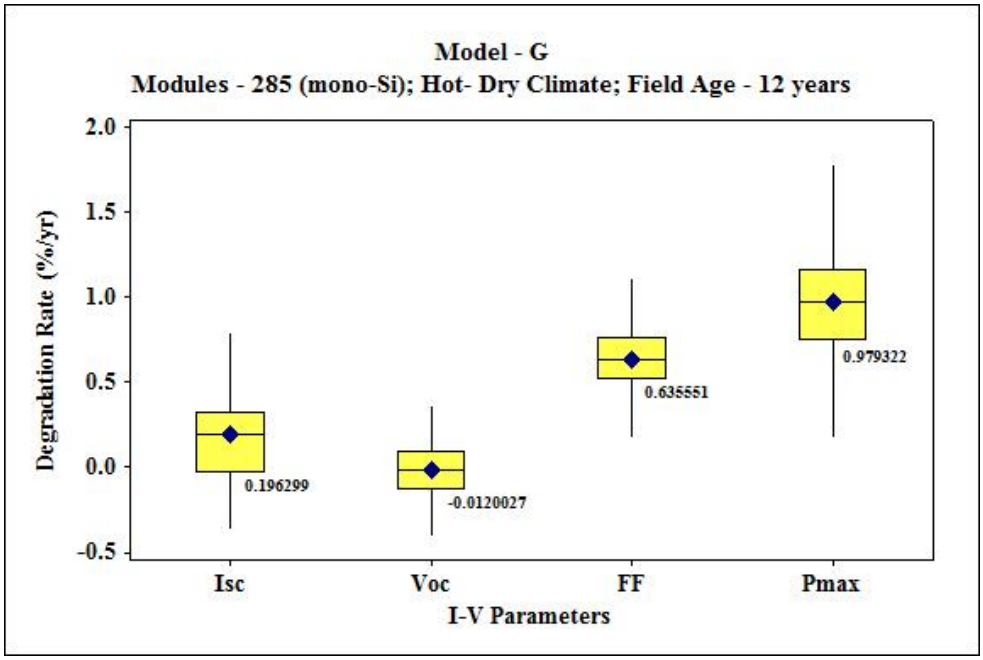

Figure 43. Box plot of I-V parameter degradation rates for Model –G

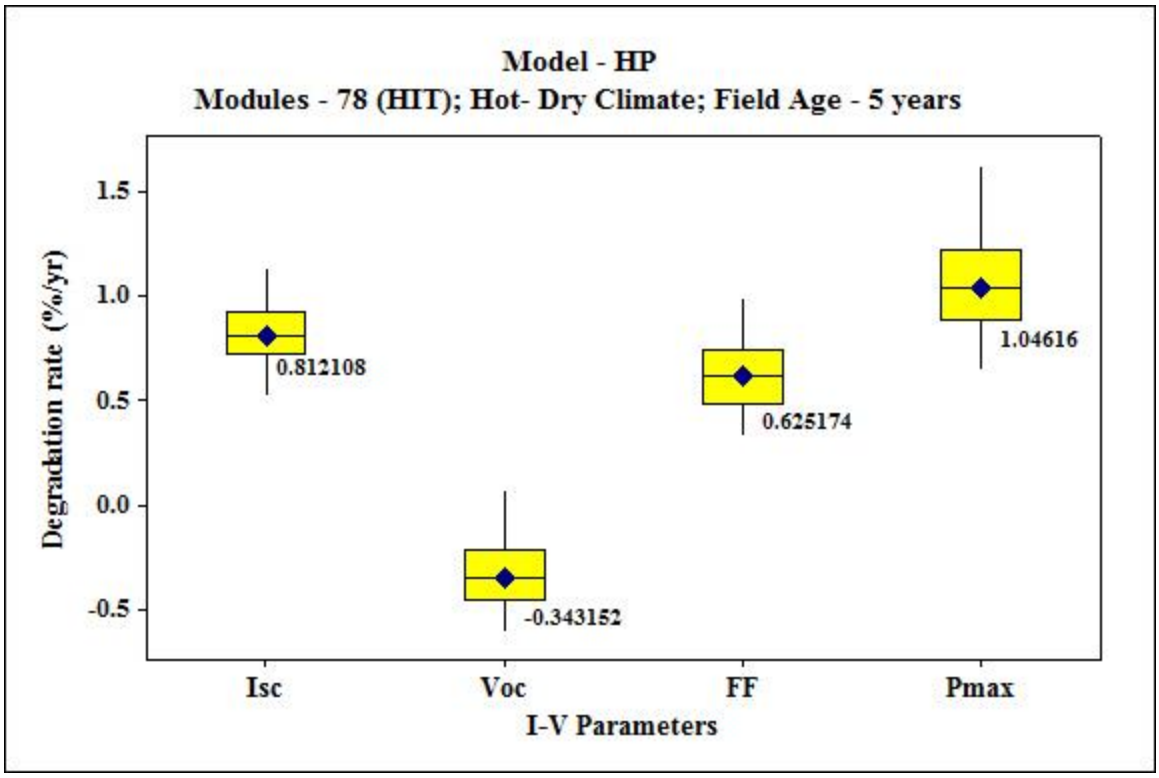

Figure 44. Box plot of I-V parameter degradation rates for Model –HP

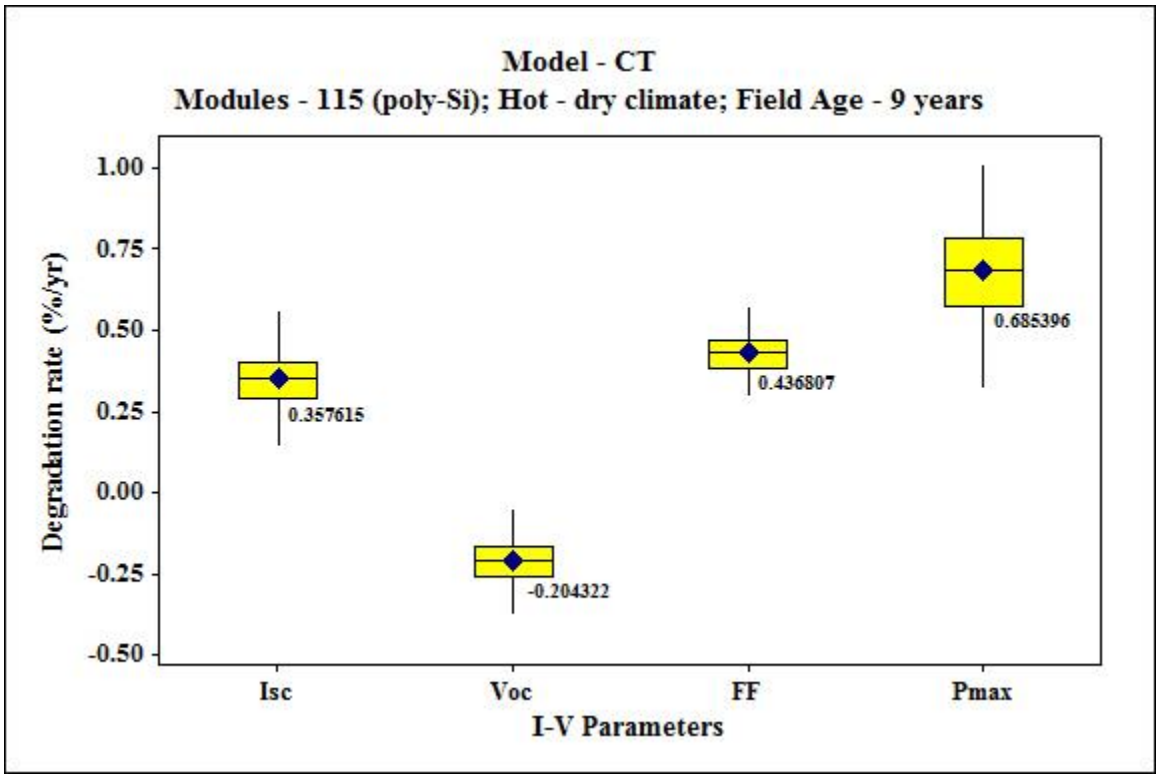

Figure 45. Box plot of I-V parameter degradation rates for Model –CT

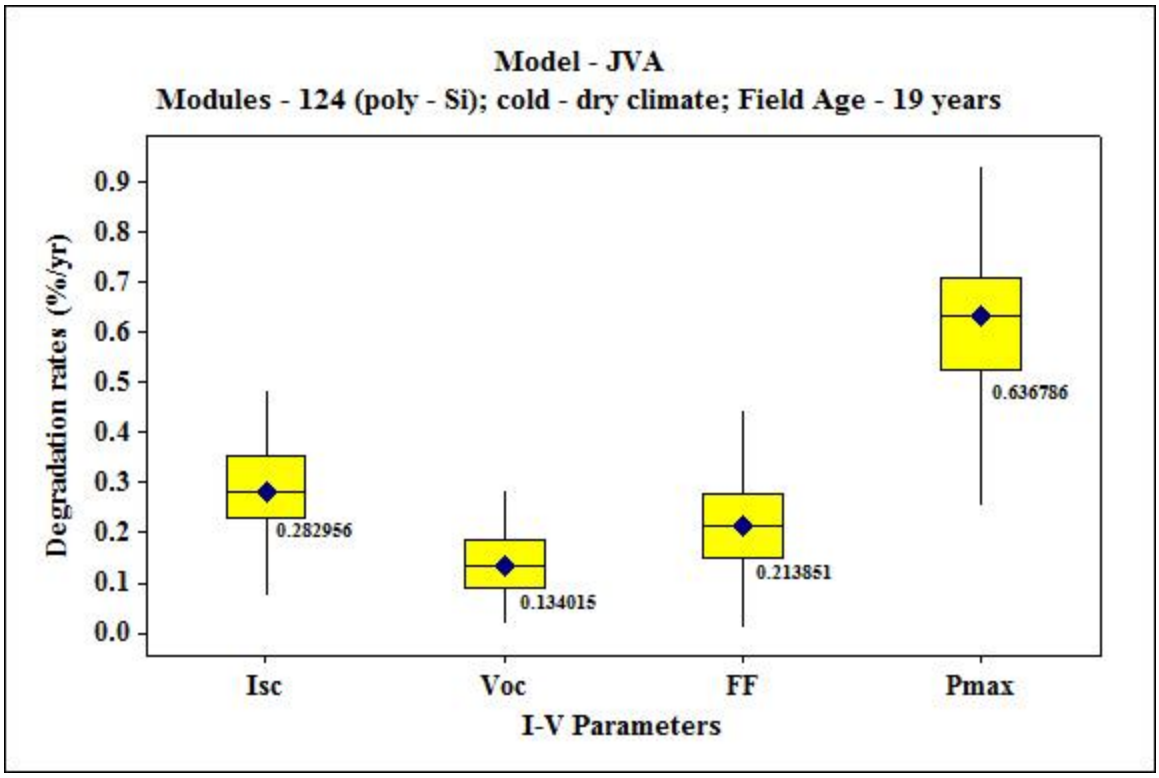

Figure 46. Box plot of I-V parameter degradation rates for Model – JVA

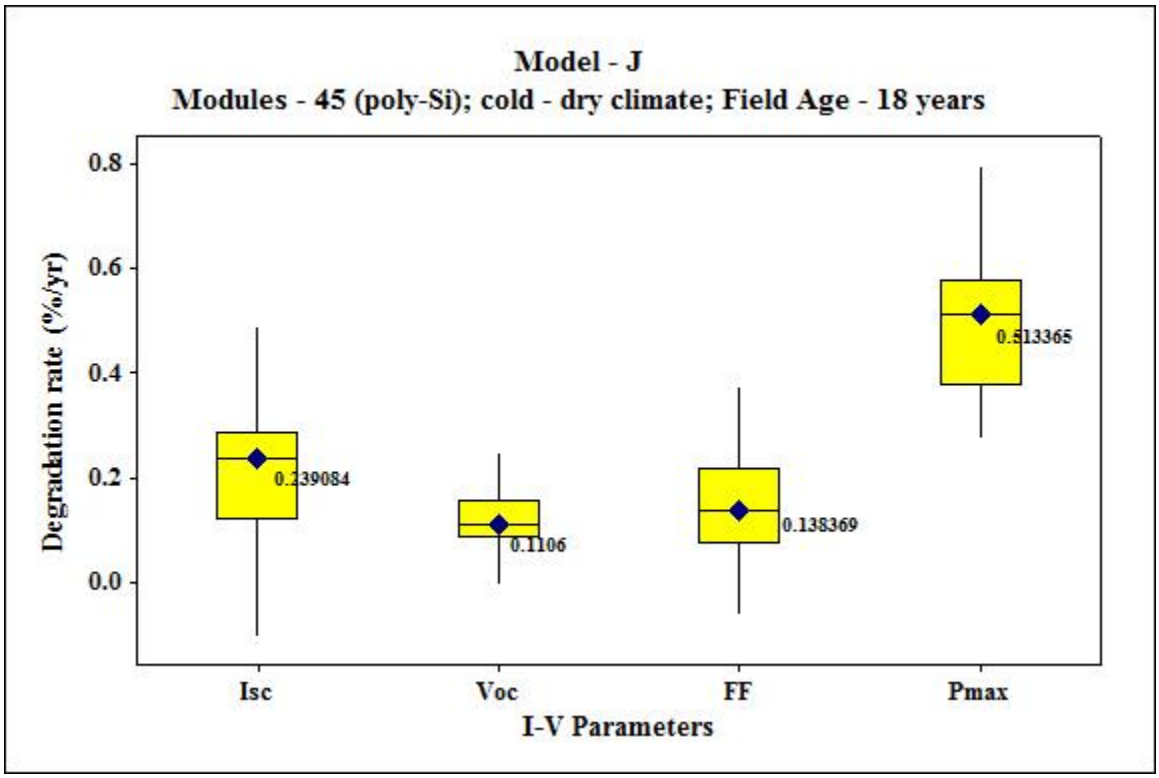

Figure 47. Box plot of I-V parameter degradation rates for Model – J

Scatter plots comparing degradation rates for Pmax, Isc, Voc and FF are given in APPENDIX B.

2.4.2.2 **Hypothesis Testing**

Hypothesis testing, a statistical test of significance, is done on the degradation rates of I-V parameters. Isc, Voc, and FF were tested to identify the significant parameter affecting Pmax. Table 6 shows the statistical order of influencing parameters which is obtained after performing the hypothesis test.

TABLE 6

Statistical order of significance

MODEL	Module type	Climate	Statistical order of significance
Model G (Frameless)	mono - Si	Hot - Dry	Voc = Isc < FF
Model HP (Framed)	Mono – Si (HIT)	Hot - Dry	Voc < FF < Isc
Model CT (Framed)	Poly - Si	Hot - Dry	Voc < Isc < FF
Model J (Frameless)	Poly - Si	Cold - Dry	FF = Voc < Isc
Model JVA (Framed)	Poly - Si	Cold - Dry	Voc < FF < Isc

From Table 6 and Figure 48, it is evident that fill factor losses are high in the hot-dry climate while Isc losses are high in cold-dry climate.

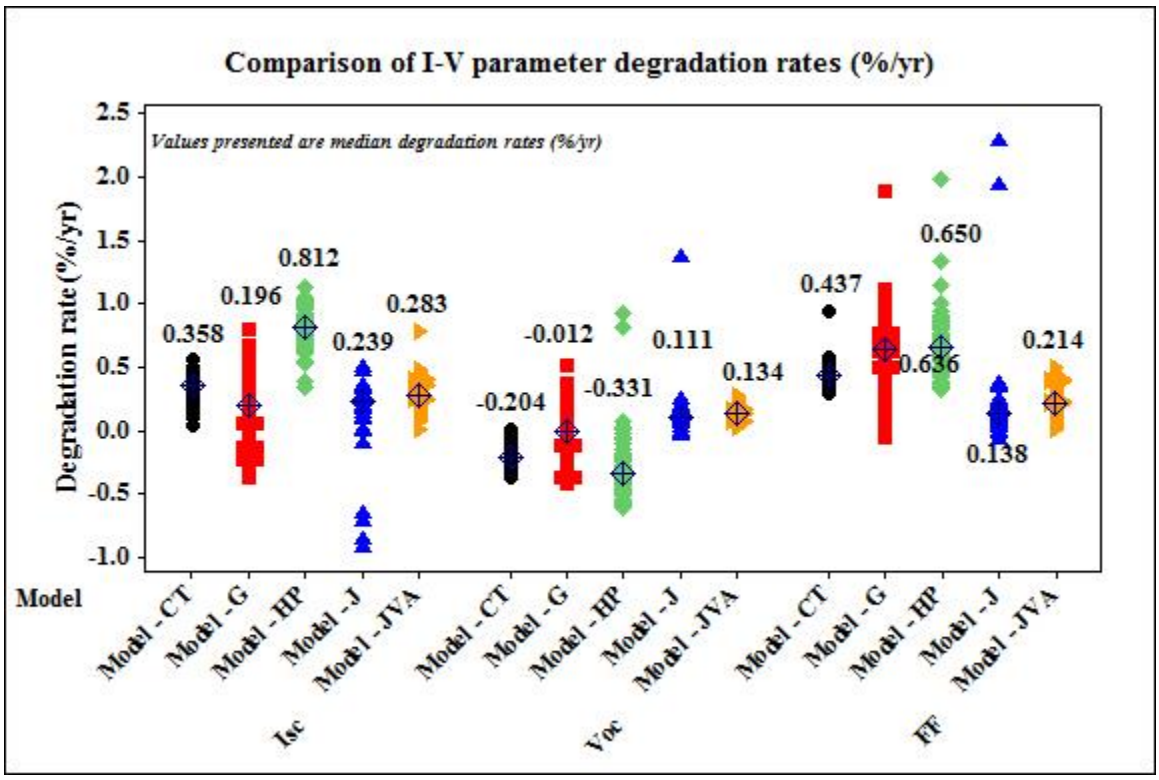

Figure 48. Comparison of Isc, Voc and FF degradation rates for all models

It is to be noted that the Voc loss is significant in cold-dry climate, especially for the frameless modules, due to triggering of bypass diodes because of current mismatch between the cells caused by encapsulant delamination over a few cells. It is also to be noted that Model-HP had higher Isc degradation rate than the other technologies in the same hot-dry climate, and this is attributed to the difference in module technology (HIT) and backsheet discoloration at the inter-cell areas. Since the HIT technology is a hetero-junction c-Si technology with a top a-Si layer, it is suspected that the higher Isc loss in this technology is partly due to the initial degradation (Staebler - Wronski effect) of a-Si layer. Since the inter-cell area is yellow discolored (probably due to UV penetration

through glass and encapsulant), the higher Isc degradation in these modules could also be attributed to the reduction in backsheet scattered light contribution to Isc. Figure 49 shows Rs and Rsh degradation comparison. The series and shunt resistances were calculated from the slopes of the I-V curves at near Voc and Isc, respectively.

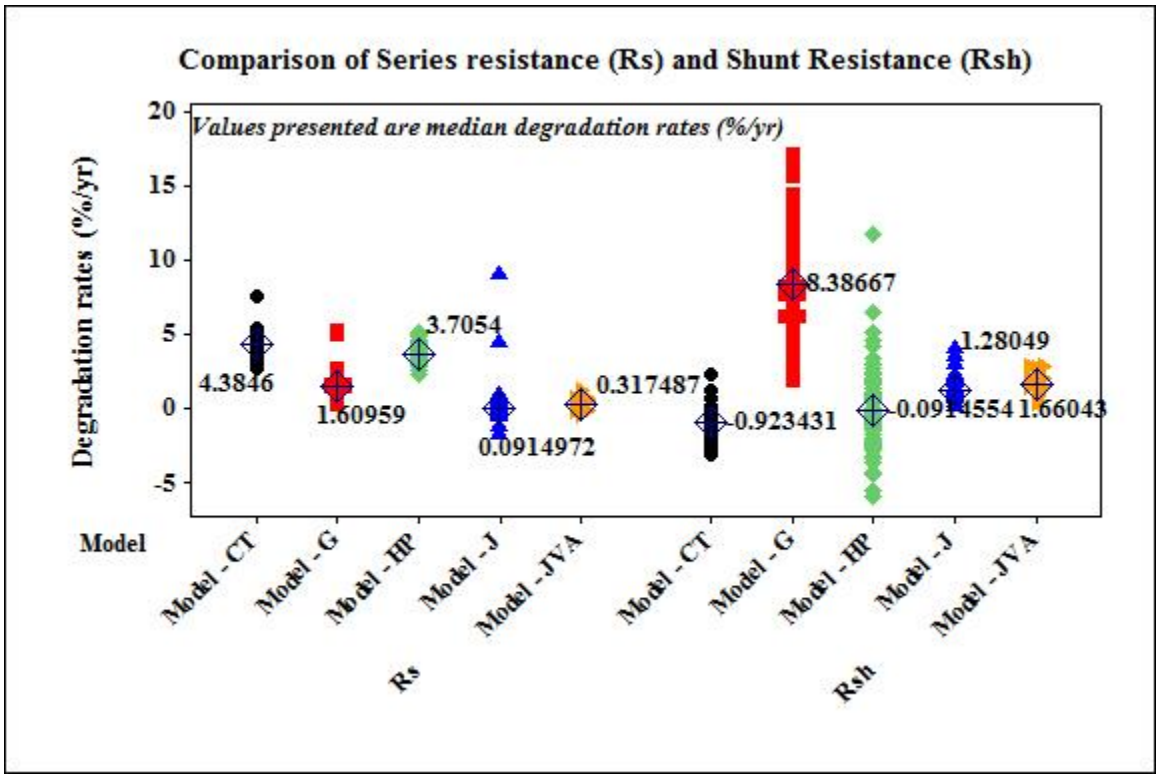

Figure 49. Comparison of series and shunt resistances for all models

It can be inferred from Figure 49 that the series resistance tends to degrade at higher rate (i.e. Rs tends to increase at higher rate) in hot-dry climates as compared to cold-dry climates. The higher degradation of Rs in hot-dry climate as compared to cold-dry climate could be attributed to higher thermo-mechanical fatigue caused by the higher temperature operating regime of these modules. The outliers shown in Figure 49 for the series resistance are attributed to the encapsulant delamination causing current mismatch leading to bypass diode triggering with change in slope at near Voc. The extent of

vertical spread of shunt resistance degradation provides a clear indication of cell/junction tolerance quality control during manufacturing or junction quality change during field exposure. Model-CT, Model-J and Model-JVA experience a very small vertical spread in Figure 49 indicating a good quality control of these c-Si modules during manufacturing. The higher vertical spread of Model-G is attributed to poor quality control of these c-Si modules during manufacturing. The higher vertical spread of Model-HP is attributed to the junction quality change during field exposure as these modules are based on the hetero-junction technology with mono-Si/a-Si junction.

2.4.3 **Correlation between Defects and I-V Parameter Degradation**

Correlation plots of visual defects with I-V parameters for all the models are discussed below. These plots are useful to identify: first, the most dominant defect that is responsible to the highest degradation rate of a specific I-V parameter; and second, the most dominant defect that is responsible for the proportional variation of degradation rate of a specific I-V parameter. The determination for the first identification can be made using the median value of the degradation rates of individual I-V parameters and for the second identification can be made using the extent of vertical spread and density of the degradation rates of individual I-V parameters.

Model G: The dominant defect for a plant is determined from the graphs shown below where module I-V parameters and defects are plotted together and by the process of elimination few defects are neglected, eventually identifying the dominant defect for each parameter and for the whole plant. Figure 50 show the defects mapped with I-V parameter for model – G and similar plots are given below for other plants. For the FF degradation of Model-G, the defects have the effect on the median degradation in the

following order: ID = ED = EY > EB > DF > R-R-SBF. Similarly, the defects have the effect on the vertical degradation rate spread in the following order: ID >> DF >> ED >> EB = R-R-SBF. Since FF is not expected to be significantly affected by ED, EY, EB, DF, R-R-SBF in this specific module design, it is determined, by process of elimination, that ID (interconnect discoloration) is the most probable defect responsible for the FF degradation in this power plant.

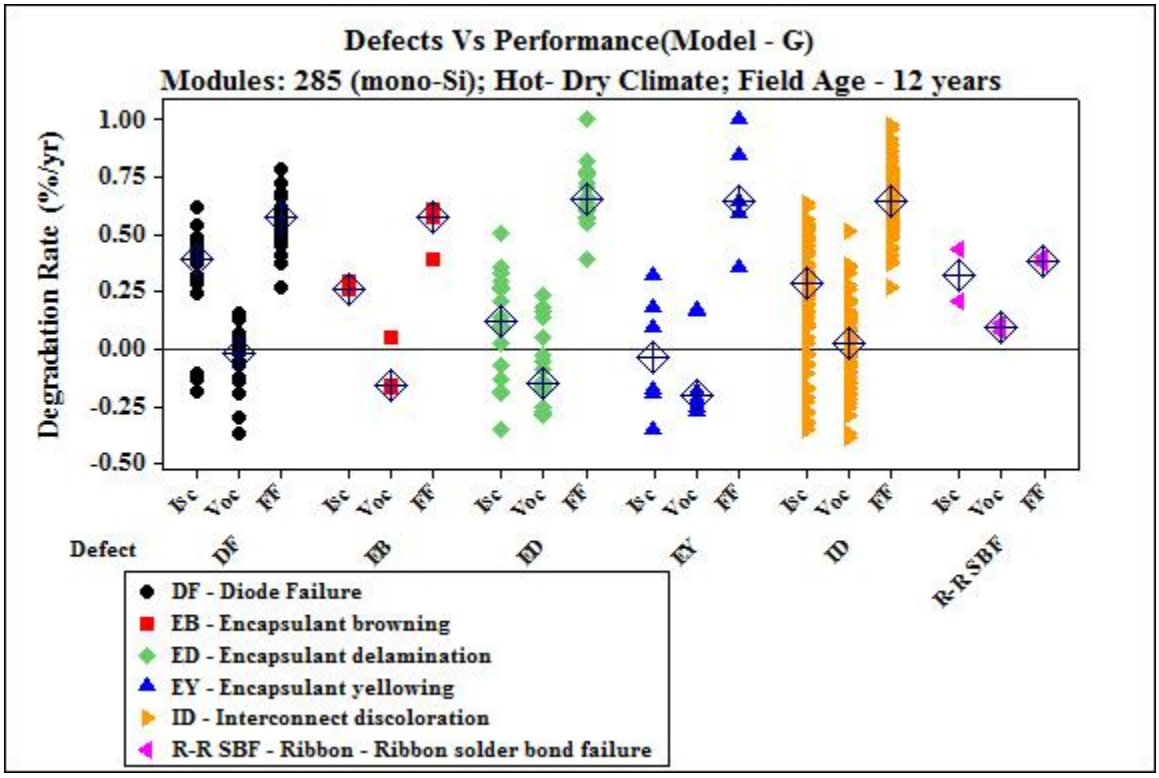

Figure 50. Defect vs degradation rates of I-V parameters for model - G

For the Voc degradation of Model-G, none of the defects have significant effect on the median degradation rate (close to zero) and vertical degradation rate spread. Since Voc cannot be significantly affected by any of these defects in this specific module design, it is determined, by process of elimination, that none of these defects is responsible for the Voc degradation in this power plant. For the Isc degradation of

Model-G, the defects have the effect on the median degradation in the following order: DF > ID = EB = R-R-SBF >> ED = EY. Similarly, the defects have the effect on the vertical degradation rate spread in the following order: ID >> ED > DF >> EB = = EY = R-R-SBF. By process of elimination, the ID (interconnect discoloration) and ED (encapsulant delamination) are determined to be the most probable defects responsible for the Isc degradation in this power plant. Figure 51 to 54 also show similar plots for other plants.

Model - HP:

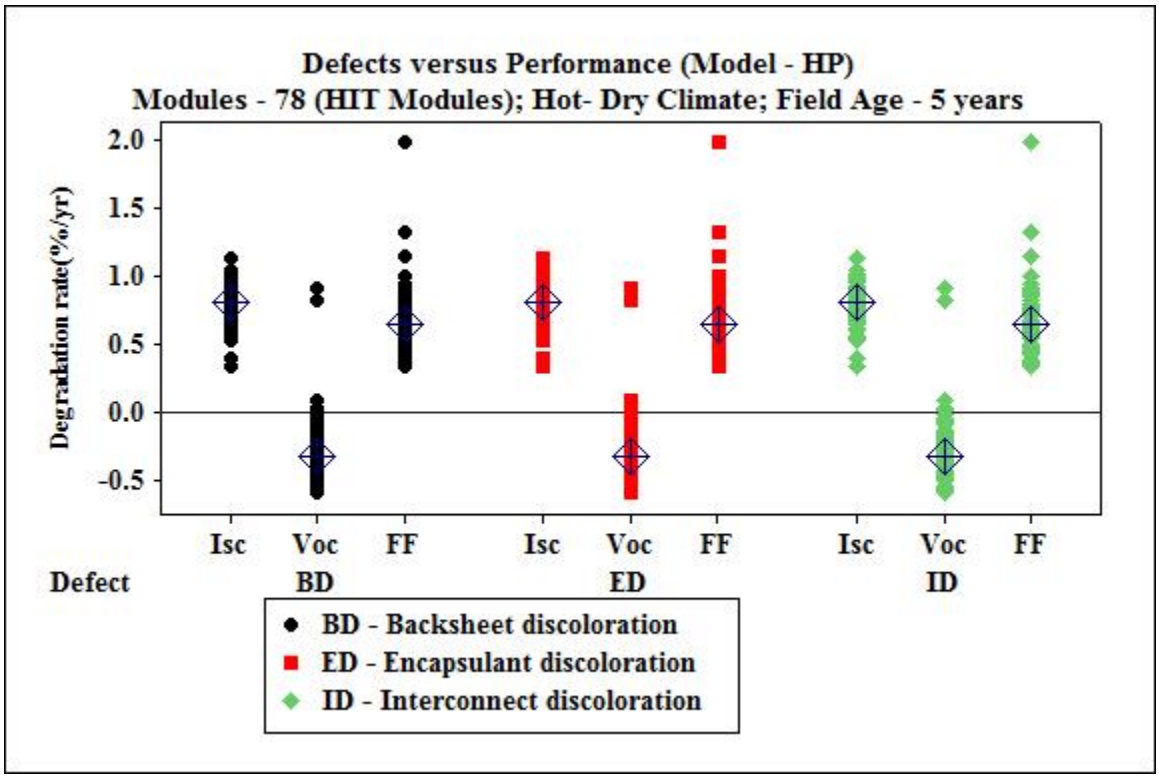

Figure 51. Defect vs degradation rates of I-V parameters for model – HP

Interconnect discoloration caused due to solder bond issue, backsheet discoloration and slight encapsulant discoloration on top of junction box are reasons for performance loss in this plant. Higher fill factor losses are caused due to interconnect

discoloration/solder bond issues. It is also seen that there are higher Isc losses and this could be either because of the module technology (HIT) or due to backsheet discoloration.

Model - CT:

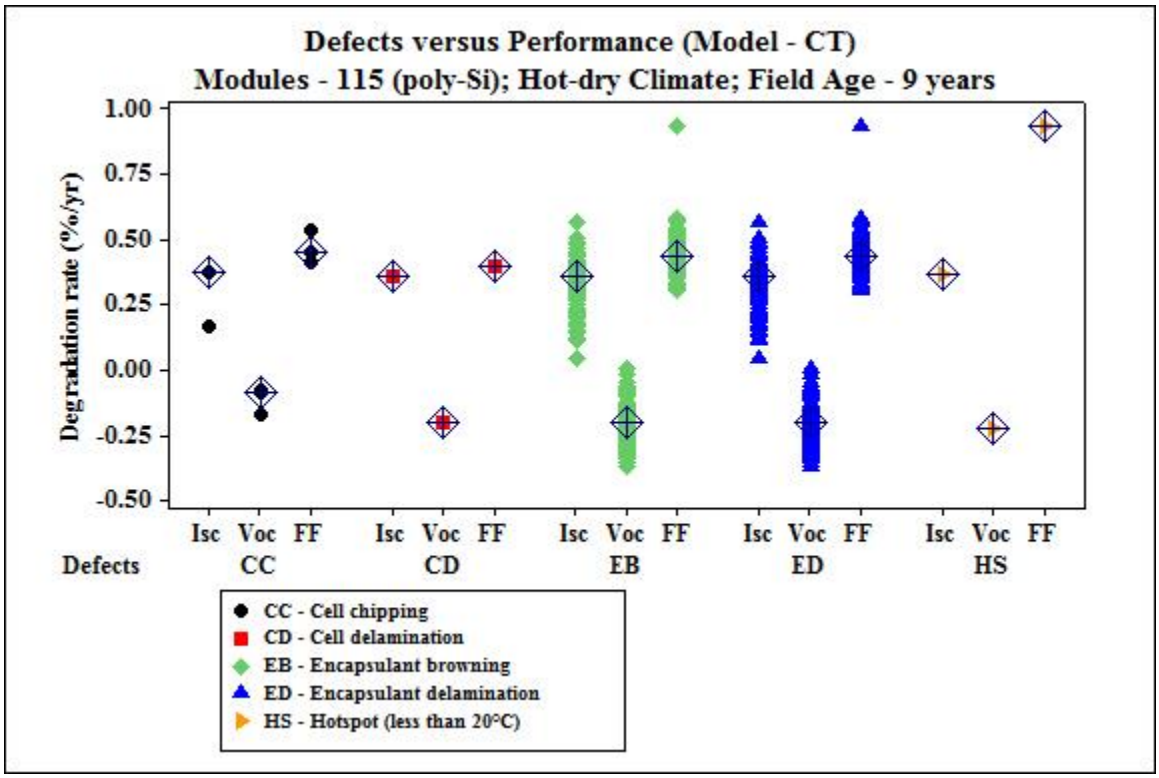

Figure 52. Defect vs degradation rates of I-V parameters for model – CT

Encapsulant was a major issue in this plant, almost all the modules had encapsulant delaminated near the fingers/gridlines along with discolored encapsulant leading to higher Isc losses. Although there were Isc losses, fill factor seems to be degradation more than Isc and there is about 38% average series resistance increase in all the modules in consideration for this plant.

Model - J:

Two main visual defects contributed to performance losses in this plant, backsheet bubbles, and encapsulant delamination over the cell and near the edges. There were also considerable number of modules in which moisture penetration was visible. Encapsulant delamination could have led to optical decoupling causing loss of Isc as well as Voc.

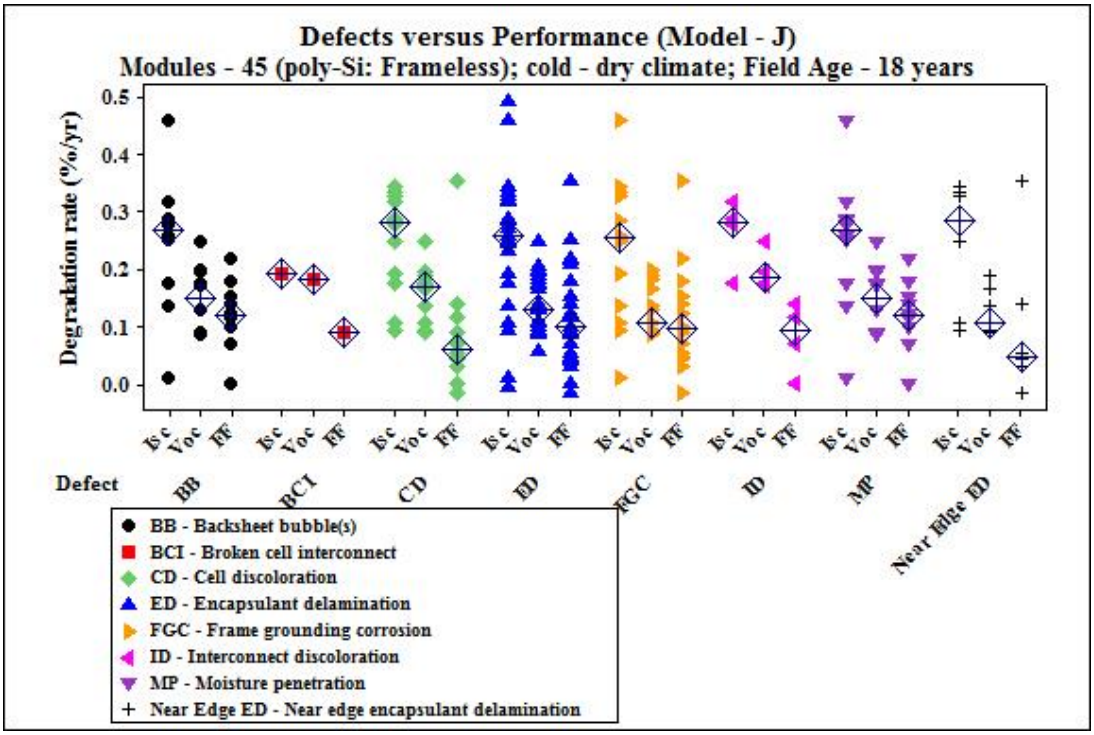

Figure 53. Defect vs degradation rates of I-V parameters for model – J

During visual inspection it was found that in, about 2% of modules in which diodes failed had delamination as well. This indicates that frameless modules are very susceptible to moisture in cold-dry climate.

Model – JVA:

Encapsulant browning and interconnect discoloration are the dominant defects in model – JVA. . We also found modules with moisture penetration which could have led to backsheet delamination and bubbles.

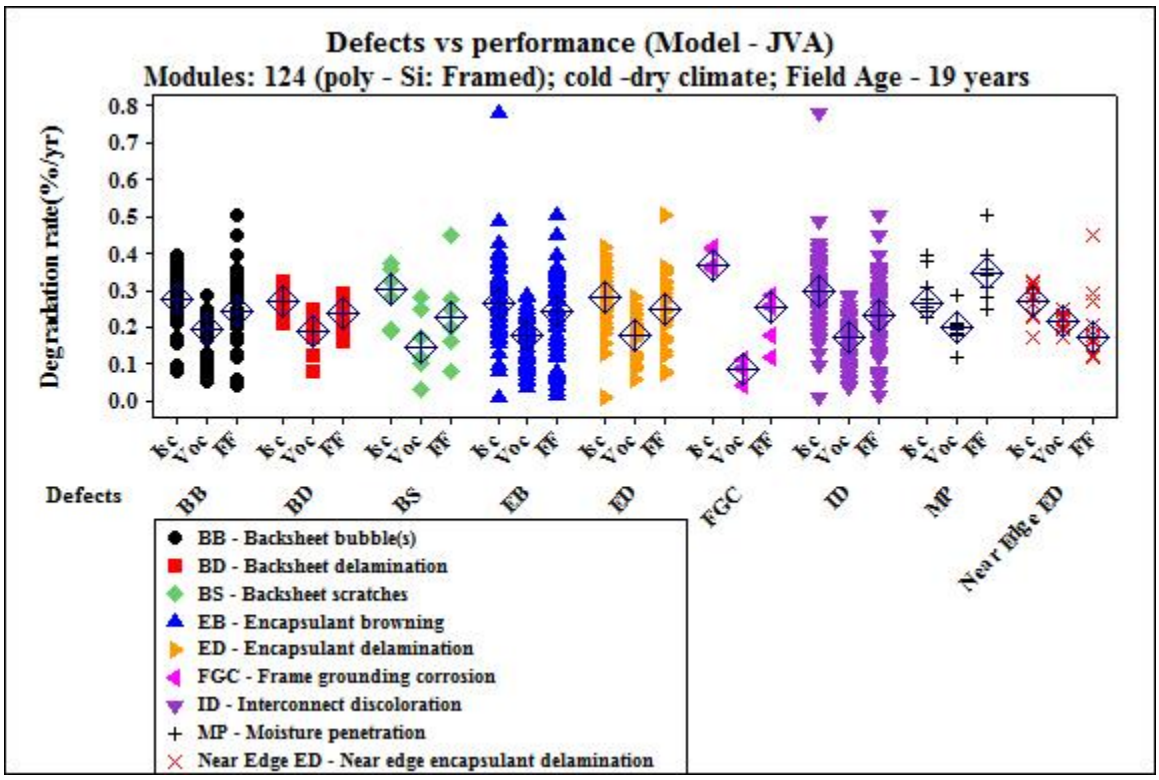

Figure 54. Defect vs degradation rates of I-V parameters for model – JVA

2.5 **CONCLUSION**

In this second part of the thesis, an analysis of field data obtained from old PV power plants was performed using various statistical techniques to identify the most influential degradation modes in two different climates: hot-dry (Arizona); cold-dry (New York). The affected performance parameters (Isc, Voc, FF and Pmax) were then correlated with the defects to determine the most dominant defect affecting power degradation. Overall, this analysis concludes that the cell interconnect discoloration (or solder bond deterioration) is the dominant defect in hot-dry climate leading to series resistance increase and power loss, while encapsulant delamination is being the most dominant defect in cold-dry climate leading to cell mismatch and power loss. In hot-dry climate, fill factor is typically the most affected parameter due to series resistance increase because of solder bond degradation, metallization degradation and/or interconnect discoloration. In cold-dry climate, Isc is typically the most affected parameter due to encapsulant delamination and discoloration.

Also, this analysis clearly indicates that the over-cell non-uniform encapsulant delamination can lead to series of cascade effects: cell-to-cell current mismatch → by-pass diode triggering → loss of entire cell-string voltage and hence loss of entire cell-string power (performance loss) → daily and continuous by-pass diode operation over several years leading permanent failure under open circuit condition (performance regain) → hotspot generation on the encapsulant delaminated cells due to cell reverse bias → backskin burning → safety hazard (electrical and/or fire hazard).

REFERENCES

1. ASTM E1036-15, Standard Test Methods for Electrical Performance of Nonconcentrator Terrestrial Photovoltaic Modules and Arrays Using Reference Cells , ASTM International, West Conshohocken, PA, 2015, www.astm.org

2. International Electrotechnical Commission, IEC 61853-1 Ed.1: "Photovoltaic (PV) module performance testing and energy rating – Part 1: Irradiance and temperature performance measurements and power rating", 2011.

3. E. E. van Dyk, B. J. Scott, E. L. Meyer, and A. W. R. Leitch, "Temperature dependence of performance of crystalline silicon photovoltaic modules", South African Journal of Science, vol. 96, pp.198 -200, 2000.

4. E.L. Meyer and E.E. van Dyk, "Assessing the Reliability and Degradation of Photovoltaic Module Performance Parameters," IEEE Trans. Reliability, 53, pp. 83-92, 2004.

5. David Faiman, "Assessing the Outdoor Operating Temperature of Photovoltaic Modules". Progress in Photovoltaics: Research and Applications,16, pp. 307-315, 2008

6. K. Emery et al. "Temperature dependence of photovoltaic cells, modules and systems", 25th IEEE PVSC, pp. 1275-1278, 1996.

7. D. L. King et al., "Temperature Coefficients for PV Modules and Arrays: Measurement Methods, Difficulties, and Results", 26th IEEE Photovoltaic Specialists Conference, 1997.

8. D.L. King, "Photovoltaic Module and Array Performance Characterization Methods for All System Operating Conditions", Proceeding of NREL/SNL Photovoltaics Program Review Meeting, November 18-22, 1996, Lakewood, CO, AIP Press, New York, 1997.

9. International Electrotechnical Commission, IEC 61853-2 "Photovoltaic (PV) module performance testing and energy rating – Part 2: Spectral response, incidence angle and module operating temperature measurements" (draft)

10. Kurnik, J., Jankovec, M., Brecl, K., Topic, M., 2011. Outdoor testing of PV module temperature and performance under different mounting and operational conditions. Sol. Energy Mater. Sol. Cells 95, 373–376, 2010

11. R. Bharti, J. Kuitche, and M.G. TamizhMani. Nominal Operating Cell Temperature (NOCT): Effects of module size, loading and solar spectrum in Photovoltaic Specialists Conference (PVSC), 2009 34th IEEE. 2009

12. Tang Y, TamizhMani G, Ji L, Osterwald C. Outdoor energy rating of photovoltaic modules. Proceedings of 20th European Photovoltaic Solar Energy Conference, Barcelona, 2005; in print.

13. Bo Li, Master's thesis: Outdoor photovoltaic module performance measurements-Implementation of Sandia National Laboratories method and improvement of thermal test bed, 2006

14. G.TamizhMani, L. Ji, Y. Tang and L. Petacci, "Photovoltaic Module Thermal/Wind Performance: Long -Term Monitoring and Model Development for Energy Rating," in NCPV and Solar Program Review Meeting, 2003.

15. Jones AD, Underwood CP. A thermal model for photovoltaic systems. Solar Energy 2001; 70:349‑59.

16. M. A. Quintana, D. L. King, T. J. McMohan, and C. R. Osterwald,"Commonly observed degradation in field-aged photovoltaic modules," 29th IEEE Photovoltaic Specialist Conference, New Orleans, LA, USA, 2002, pp. 1436‑1439.

17. G. TamizhMani, J. Kuitche, "Accelerated Lifetime Testing of Photovoltaic Modules Solar America Board for Codes and Standards," A report of Solar America Board for Codes and Standards (solarabcs.org), 2013.

18. K. Olakonu, J. Belmont, J. Kuitche and G. TamizhMani, "Degradation and Failure Modes of 26-Year-Old 200 kW Power Plant in a Hot-Dry Desert Climate" in 40th IEEE Photovoltaic Specialist Conference, 2014, pp.3207 – 3210.

19. J. Mallineni, B. Knisely, K. Yedidi, S. Tatapudi, J. Kuitche and G. TamizhMani, "valuation of 12-Year Old PV Power Plant in Hot – Dry Desert Climate: Potential Use of Field Failure Metrics for Financial Risk Calculation," in 40th IEEE Photovoltaic Specialist Conference, 2014, pp. 3366 – 3371.

20. S. Chattopadhyay, R. Dubey, V. Kuthanazhi, J. J. John, C. S. Solanki,A. Kottantharayil, B. M. Arora, K. L. Narasimhan, V. Kuber, J. Vasi, A. Kumar, and O. S. Sastry, "Visual Degradation in Field-Aged Crystalline Silicon PV Modules in India and Correlation With Electrical Degradation," IEEE Journal of photovoltaics, vol. 4, pp. 1470-1476, 2014.

21. S. V. Janakeeraman, J. Singh, J. Kuitche, J. K. Mallineni, G. TamizhMani, "A Statistical Analysis on the cell parameters Responsible for Power Degradation of Fielded PV Modules in a Hot-Dry Climate," in 40th IEEE Photovoltaic Specialist Conference, 2014, pp. 3234 – 3238.

22. C. E. Packard, J. H. Wohlegemuth, and S. R. Kurtz, "Development of a visual inspection data collection tool for evaluation of fielded PV module condition," Nat. Renew. Energy Lab., Golden, CO, USA, Tech. Rep. NREL/TP-5200-56154, Aug. 2012.

APPENDIX A

TEMPERATURE VARIATION ANALYSIS

Table A1

Temperature coefficients for all modules used for STC translation

#	Module	Isc A/°C	Voc V/°C	Imp A/°C	Vmp V/°C	FF %/°C	Pm W/°C
1.	No Insulation - Top	0.0031	-0.2028	-0.0047	-0.2013	-0.1603	-1.7762
2.	No Insulation - Bottom	0.0035	-0.2178	-0.0047	-0.2228	-0.1769	-1.9603
3.	Frame insulation - Top	0.0048	-0.1938	-0.0081	-0.1819	-0.1855	-1.7572
4.	Frame insulation - Bottom	0.0097	-0.1971	0.0095	-0.2515	-0.2019	-1.6557
5.	Frame and backsheet - Top	0.0057	-0.1789	-0.0029	-0.1897	-0.1747	-1.6240
6.	Frame and backsheet - Bottom	0.0064	-0.2290	-0.0007	-0.2406	-0.1910	-1.9378

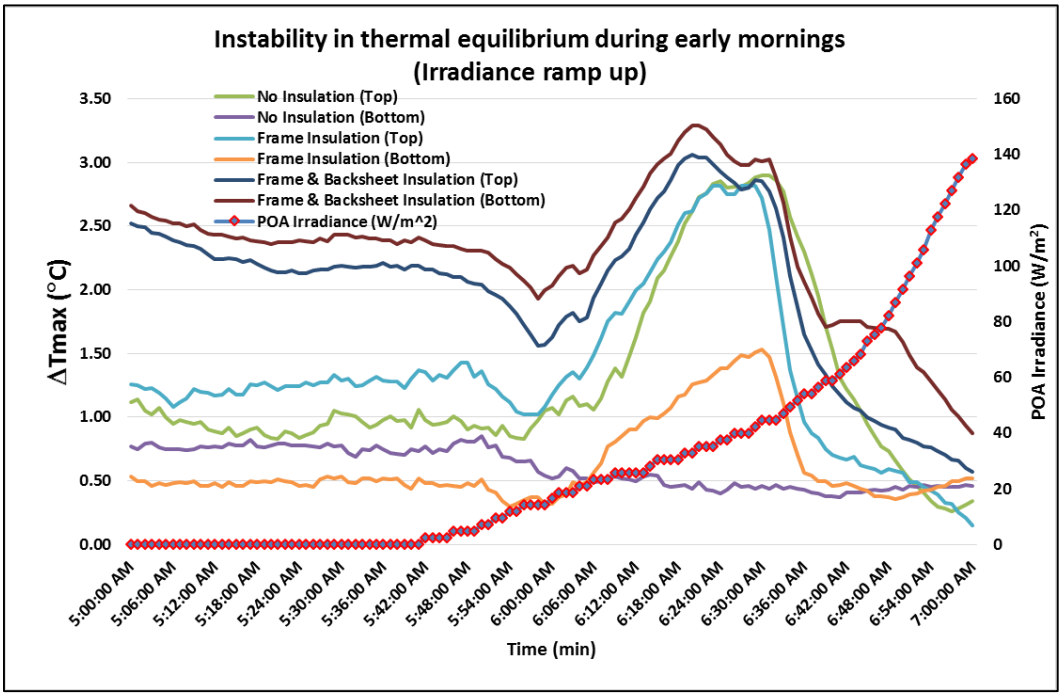

Figure A1. Thermal instability during irradiance ramp up

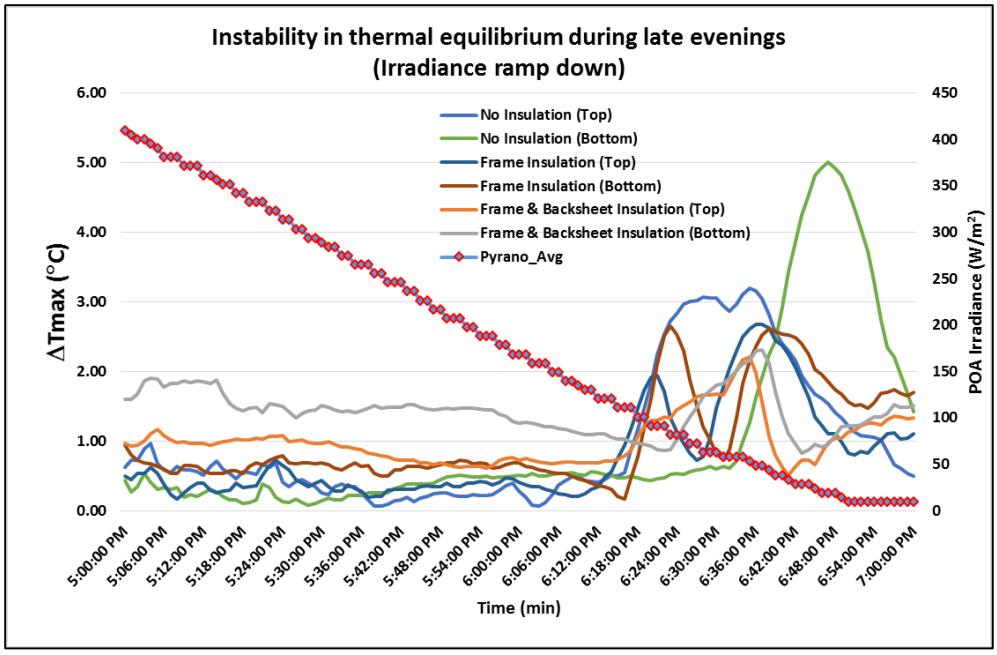

Figure A2. Thermal instability during irradiance ramp down

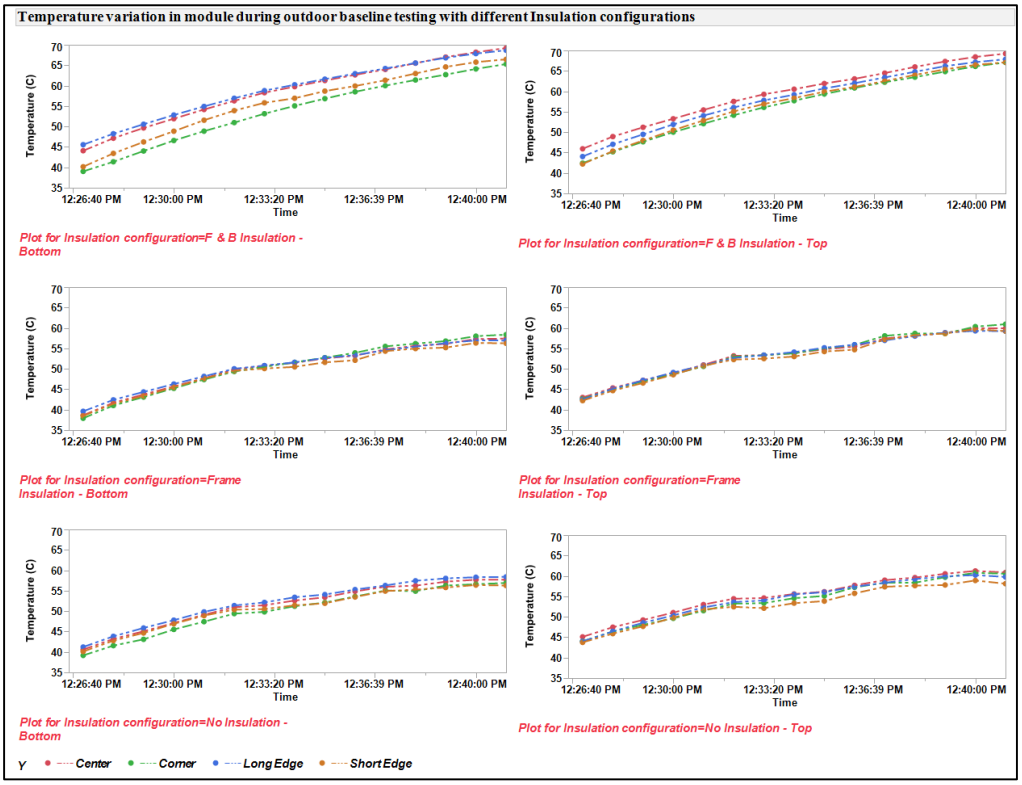

Figure A3. Temperature distribution of modules during baseline testing to obtain temperature coefficients

Table A2

Temperature coefficients for module with No Insulation

I-V Parameters	**Isc** (A/°C)	**Voc** (V/°C)	**Imp** (A/°C)	**Vmp** (V/°C)	**FF** (%/°C)	**Pm** (W/°C)
Center	0.0088	-0.1699	0.0029	-0.1851	-0.1730	-1.2831
Corner	0.0087	-0.1652	0.0029	-0.1798	-0.1681	-1.2430
Long Edge	0.0089	-0.1588	0.0033	-0.1730	-0.1622	-1.1804
Short Edge	0.0094	-0.1812	0.0033	-0.1981	-0.1843	-1.3650

Table A3

Temperature coefficients for module with Frame Insulation

I-V Parameters	**Isc** (A/°C)	**Voc** (V/°C)	**Imp** (A/°C)	**Vmp** (V/°C)	**FF** (%/°C)	**Pm** (W/°C)
Center	0.0111	-0.1580	0.0021	-0.1587	-0.1592	-1.1189
Corner	0.0110	-0.1514	0.0024	-0.1525	-0.1527	-1.0630
Long Edge	0.0111	-0.1507	0.0027	-0.1523	-0.1523	-1.0529
Short Edge	0.0114	-0.1588	0.0024	-0.1594	-0.1601	-1.1152

Table A4

Temperature coefficients for module with Frame and Backsheet Insulation

I-V Parameters	**Isc** (A/°C)	**Voc** (V/°C)	**Imp** (A/°C)	**Vmp** (V/°C)	**FF** (%/°C)	**Pm** (W/°C)
Center	0.0110	-0.1481	0.0057	-0.1583	-0.1450	-0.9984
Corner	0.0109	-0.1382	0.0059	-0.1479	-0.1357	-0.9120
Long Edge	0.0110	-0.1419	0.0058	-0.1515	-0.1389	-0.9431
Short Edge	0.0108	-0.1337	0.0059	-0.1428	-0.1309	-0.8759

APPENDIX B

DEGRADATION RATES AND VISUAL DEFECTS

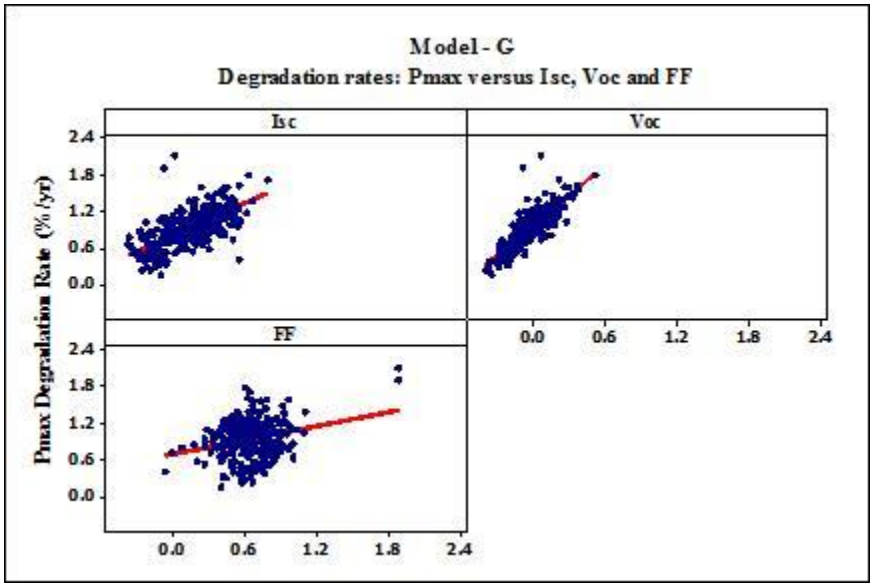

Figure B1. Pmax vs Isc, Voc and FF for model – G

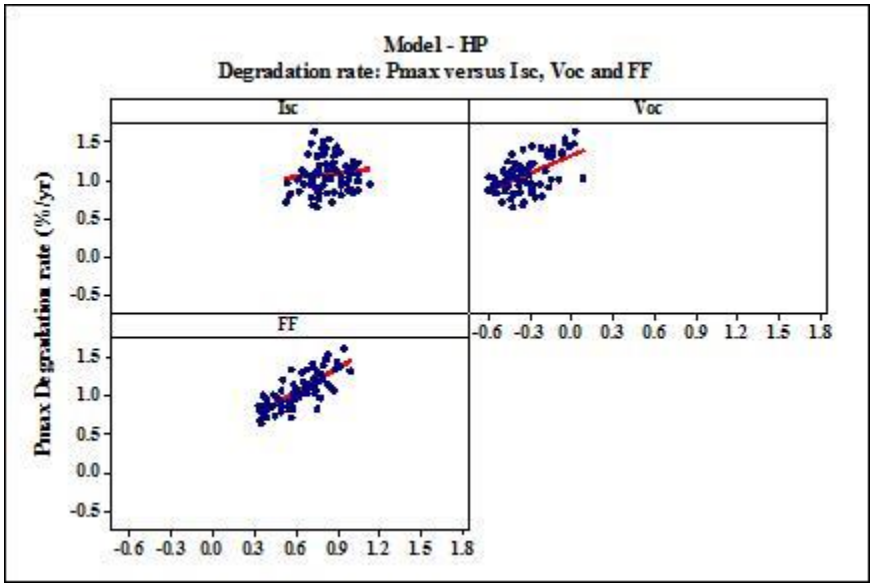

Figure B2. Pmax vs Isc, Voc and FF for model – HP

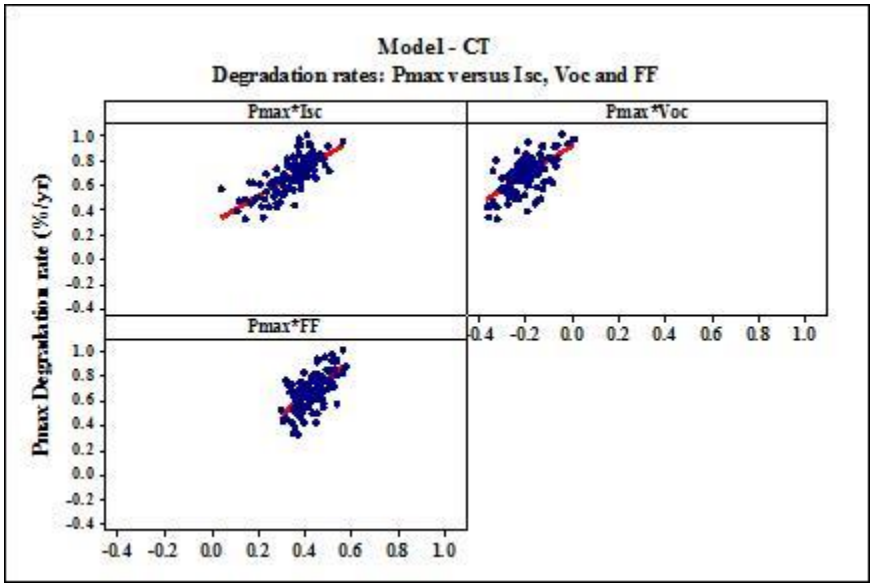

Figure B3. Pmax vs Isc, Voc and FF for model – CT

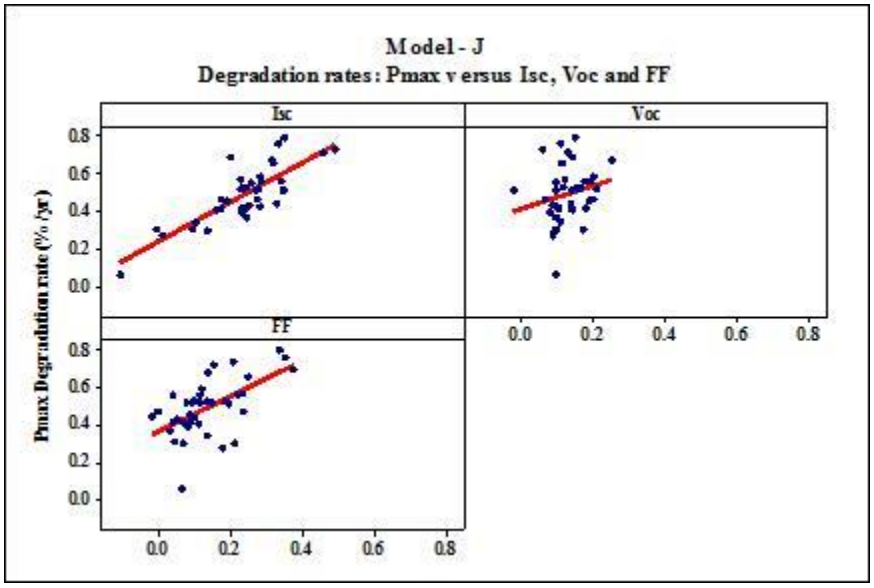

Figure B4. Pmax vs Isc, Voc and FF for model – J

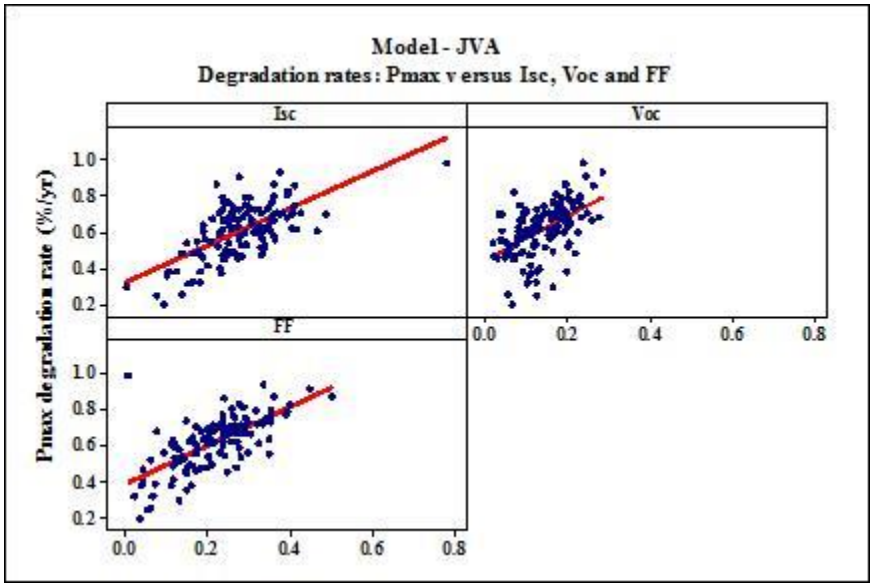

Figure B5. Pmax vs Isc, Voc and FF for model – JVA

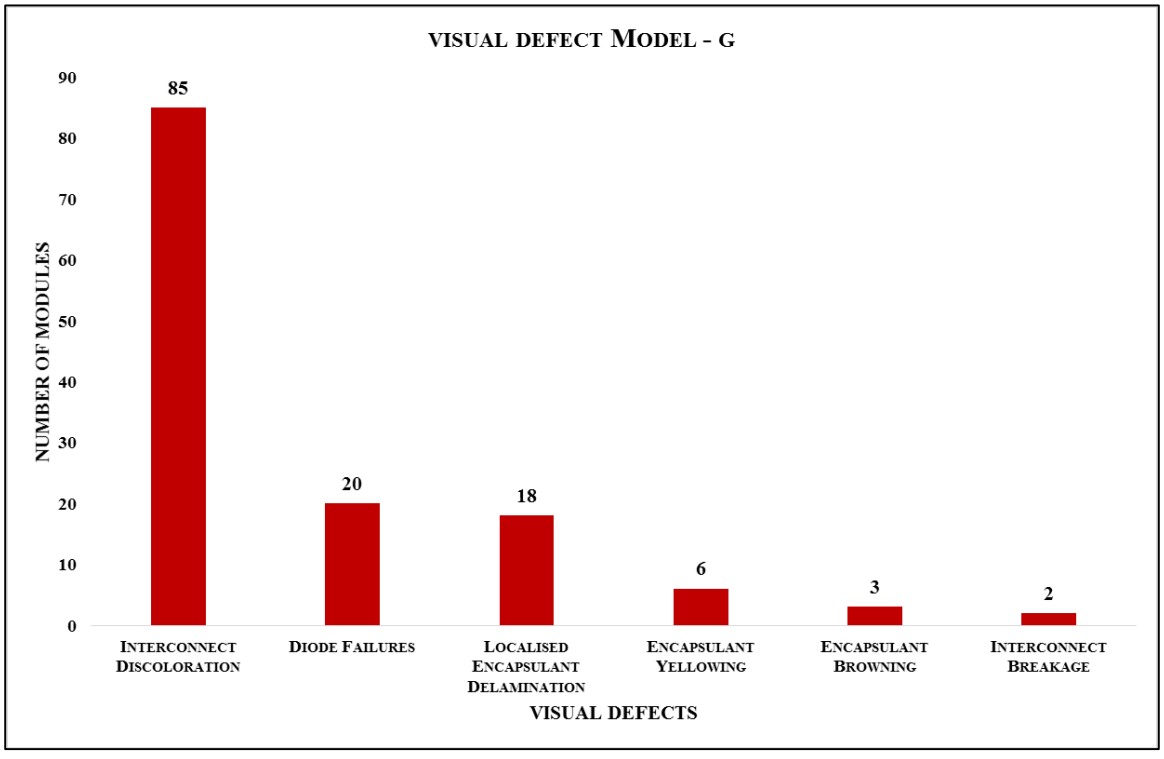

Figure B6. Visual defect chart for model – G

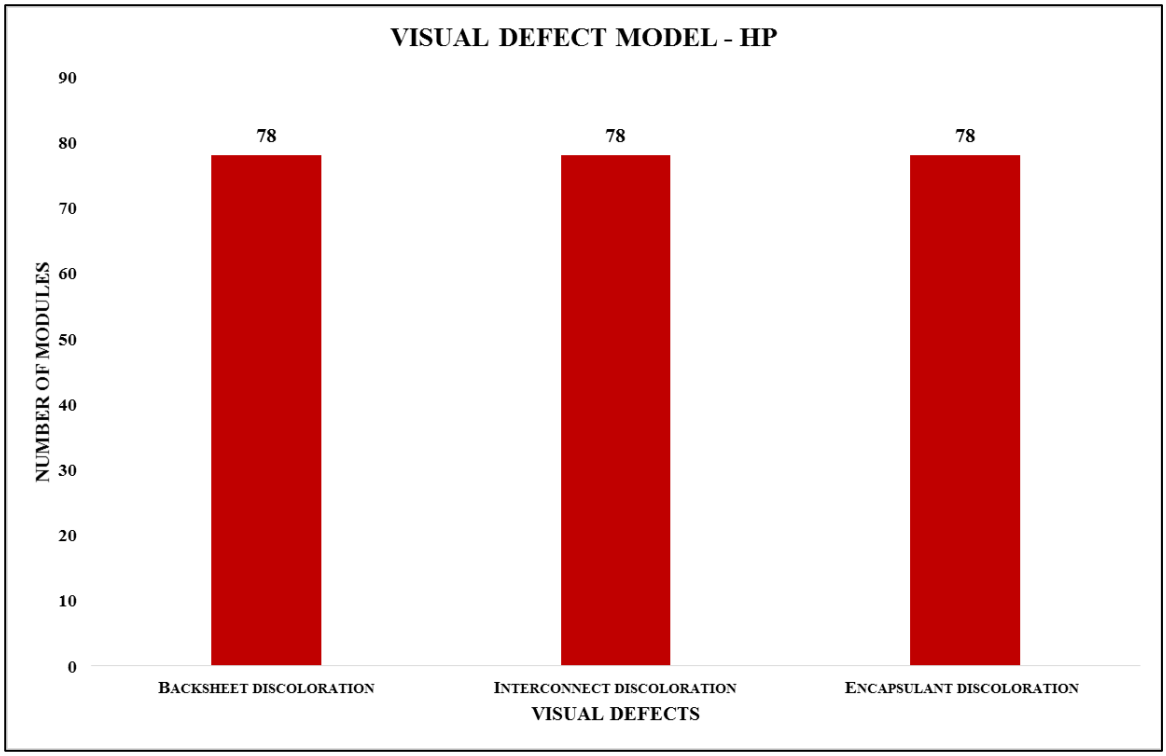

Figure B7. Visual defect chart for model – HP

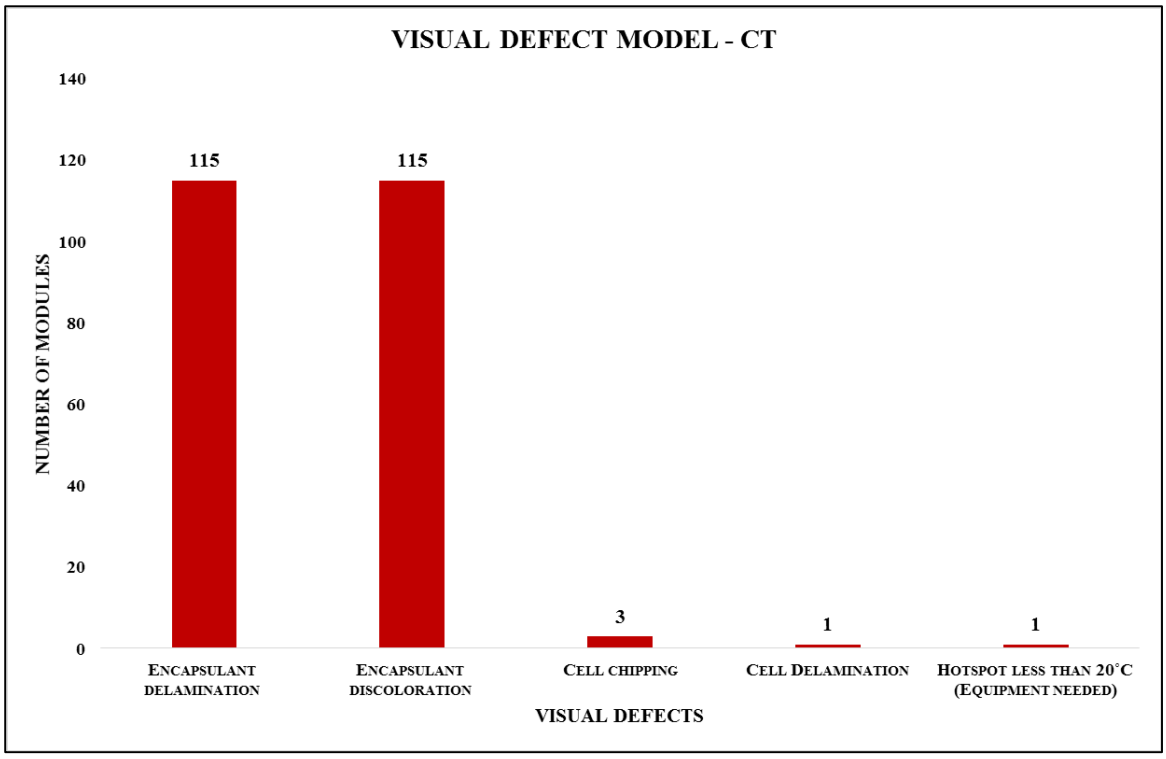

Figure B8. Visual defect chart for model – CT

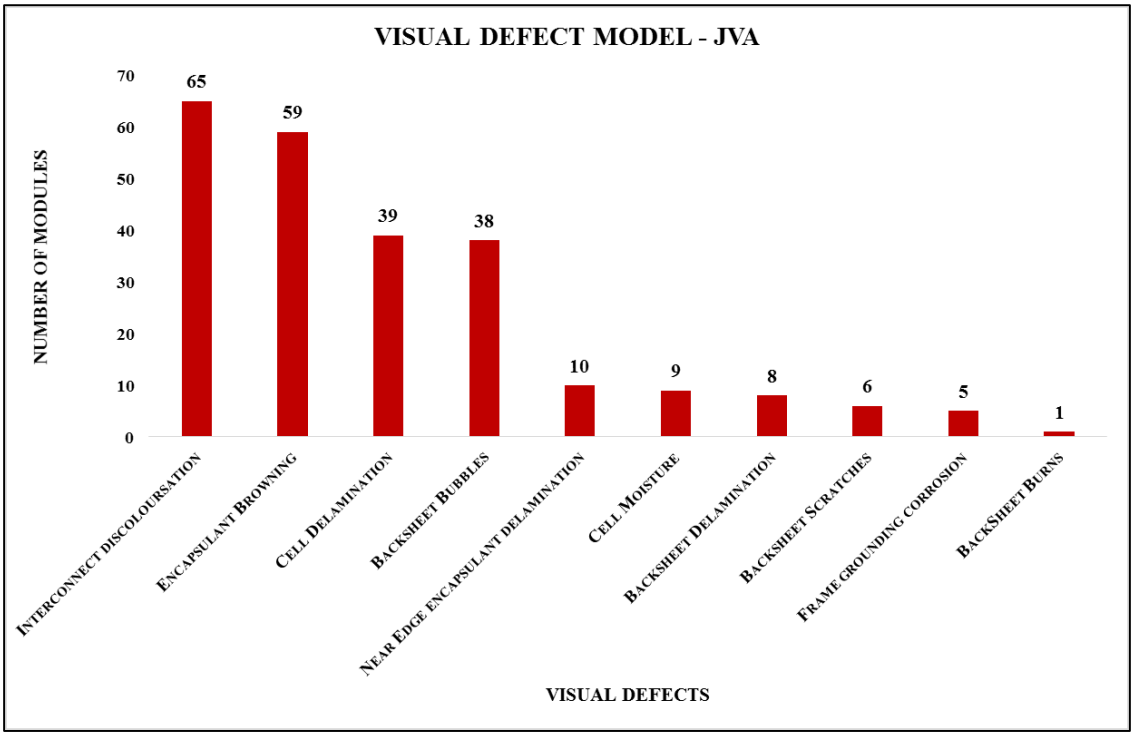

Figure B9. Visual defect chart for model – JVA

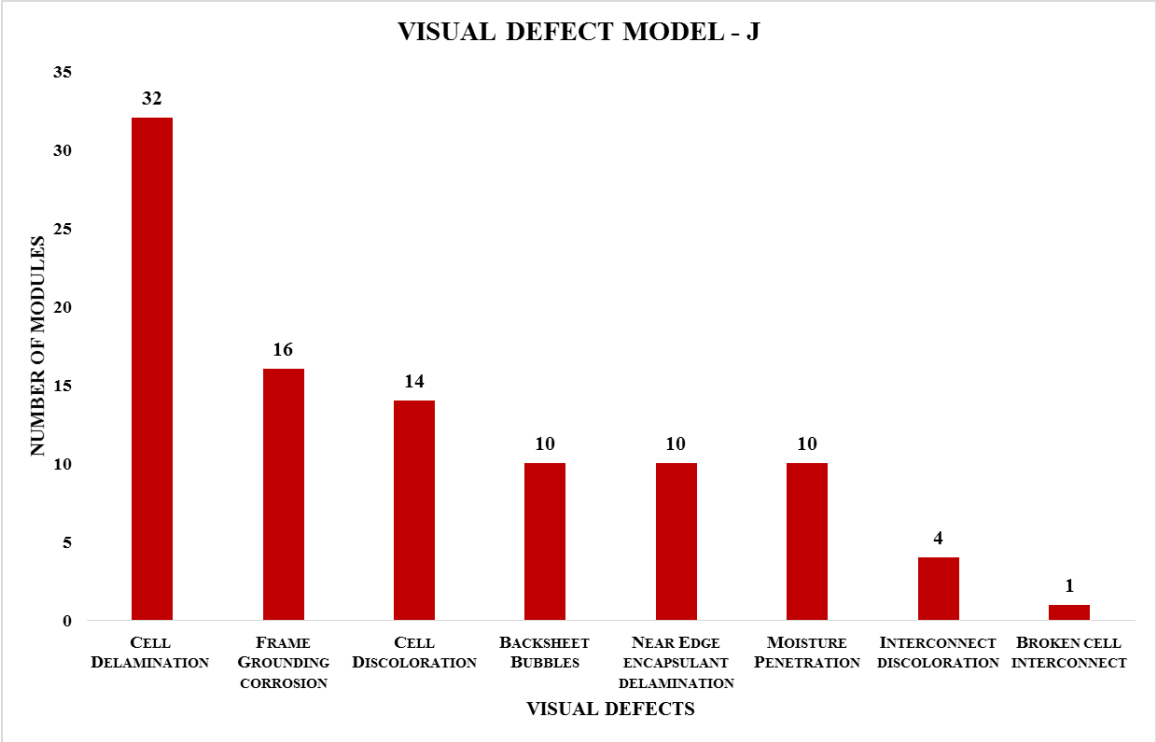

Figure B10. Visual defect chart for model – J